To my Mother.

SCATTERING BY INTERCONNECTED STRAIGHT-WIRES

by

Mohamed A.A.I. Hassan, B.Sc.(Eng.)Hons., M.Sc.(Eng.), Egypt.

Department of Electrical Engineering

McGill University,

Montreal, Canada.

SCATTERING BY INTERCONNECTED STRAIGHT WIRES

by

Mohamed A.A.I. Hassan, B.Sc.(Eng.)Hons., M.Sc.(Eng.), Egypt.

A thesis submitted to the Faculty of Graduate Studies and Research
in partial fulfillment of the requirements for the degree of
Master of Engineering.

Department of Electrical Engineering,

McGill University,

Montreal, Canada.

July, 1974.

RESUME

Une nouvelle méthode est présentée pour étudier le phénomène de dispersion d'ondes de plusieurs segments droits de conducteurs filiformes, joints arbitrairement, et irradiés par des ondes planes à polarisation linéaire.

L'équation intégrale de Pocklington qui en résulte est résolue par la méthode de projection de Bubnov-Galerkin. La répartition du courant le long des fils est approximée par des polynômes à coefficients complexes. Cette formulation est valide pour tout angle entre les segments et traite particulièrement le cas où les segments sont colinéaires. Les integrales obtenues dans cette analyse sont évaluées à l'aide de fomules de Gauss specifiquement adaptées à cette étude. Les résultats montrent un excellent accord avec ceux trouvés par d'autres chercheurs.

Un programme d'ordinateur a été mis à point afin d'analyser le comportement électromagnetique des antennes de reception. Le programme peut traiter des structures d'antennes compliquées.

ABSTRACT

A new method for treating the interconnections of arbitrarily located straight thin wires irradiated by a linearly polarized plane wave is presented. The resulting Pocklington's integral equation is solved by the Bubnov-Galerkin projective method. The current distribution along the wires is approximated by polynomials with complex coefficients. This formulation is valid for wires forming any angle, with special provision made for the collinear case. The integrals involved in the analysis are evaluated by using Gaussian quadrature formulae specially constructed for the purpose. Results show excellent agreement with those of other investigators.

A computer program was also written for the analysis of the electromagnetic behaviour of wire scatterers. The program is able to handle general wire antenna structures.

ACKNOWLEDGEMENTS

The author expresses his deep appreciation and thanks to his advisor, Professor P. Silvester, for his helpful suggestions, guidance and criticism throughout this research work. His continuous direction and encouragement made it possible for this thesis to appear in its present form.

Appreciation is also extended to Dr. B. Howarth for many helpful advices. Thanks are also due to the author's colleagues for miscellaneous discussions, and to Miss Laura Lee for her excellent typing.

Financial assistance from the National Research Council of Canada is gratefully acknowledged.

TABLE OF CONTENTS

Table of Contents (cont'd)

CHAPTER I

INTRODUCTION

To analyse the electromagnetic behaviour of any antenna, a knowledge of the current distribution is of fundamental importance. This can be obtained experimentally, but it is quite inaccurate. An exact determination of the current requires the solution to a boundary value problem which is usually formulated in terms of antenna integral equations. However, these equations are difficult to solve even for the simplest case of a dipole antenna. Therefore, numerical techniques are adopted. Examples are, Bubnov-Galerkin method, collocation method, subsectional method.

In this thesis, the Bubnov-Galerkin principle is used for the solution of Pocklington's integral equations of wire structures. Scattering by interconnected wires only is considered. The structure is illuminated by a known incident linearly polarized plane wave of arbitrary direction. The current distribution is approximated by Lagrangian interpolation polynomials with complex coefficients. The wires are assumed to be thin and made of perfect conductor and the currents flow only in the axial direction in a filamentary manner. The procedure presented here can be used to analyse linear, planar and three dimensional wire structures.

Chapter II is devoted to giving a brief review on the various numerical techniques that can be used in solving wire antennas.

In Chapter III, the application of these numerical techniques to the wire problem is explained. First, the integro-differential equation is solved using the method of subsections. Next, Hallen's equation is solved by approximating the current by polynomials with complex coefficients. Finally, the Bubnov-Galerkin projective method for solving antenna problems is presented with some details. At the end of Chapter III, a brief survey on the different methods for treating wire junctions is explained.

Chapter IV gives a complete detailed analysis for the new technique used for solving a wire antenna with interconnected elements forming any angle. The excitation matrix formulated is for analysing scattering problems only.

In the last chapfer of the thesis, numerical results obtained by solving some wire configurations of engineering interest, are clearly plotted and compared with other methods. Excellent agreement is obtained.

CHAPTER II

BASIC NUMERICAL TECHNIQUES

Approximate solutions to an operator equation can be determined by several methods. Examples are: the method of successive approximations, also called the iterative method, and the projective method.

This chapter presents a brief review on the projective method.

2.1 Projection Method

This method is used to give an approximate solution to any operator equation. It approximates the equation and then determines the exact solution for this approximating equation. Usually, this method reduces to a matrix equation, which can be solved by known techniques.

Let E and F be Banach spaces. Consider the following inhomogeneous operator equation

$$L(e) = f \qquad (2.1)$$

where L is a linear operator with domain $D(L) \subset E$ and range $R(L) \subset F$, f is the source of excitation and e is the response or the unknown function to be determined. Let $\{E_n\}$ and $\{F_n\}$ be two given subspaces,

$$E_n \subset D(L) \subset E, \quad F_n \subset R(L) \subset F \qquad (2.2)$$

Let P_n be a projection operator mapping F_n into itself, that is

$$P_n F_n = F_n \qquad (2.3)$$

and then solve

$$P_n L e_n = P_n f \tag{2.4}$$

where the sequence $\{e_1, e_2, \ldots, e_n\}$ converges to e if and only if the operator P_n maps LE_n onto F_n [11].

Equation (2.4) can be put in the form

$$P_n(Le_n - f) = 0 \tag{2.5}$$

Now, let E and F be Hilbert spaces and E_n and F_n be given subspaces spanned by $\{\varphi_i|_{i=1,2,\ldots,n}\}$ and $\{\psi_i|_{i=1,2,\ldots,n}\}$ respectively. These are subspaces of dimensionality n and are embedded in some higher dimensioned subspaces, i.e., we have to choose $\{E_n\}$ and $\{F_n\}$ such that

$$\begin{aligned} E_n \subset E_{n+k} \subset D \subset E \\ F_n \subset F_{n+k} \subset R \subset F \end{aligned} \tag{2.6}$$

The approximate solution is assumed to be the linear combination

$$e_n = \sum_{i=1}^{n} a_i \varphi_i \tag{2.7}$$

Substitution of (2.7) into (2.5) gives,

$$\sum_{i=1}^{n} P_n (L\varphi_i a_i - f) = 0 \tag{2.8}$$

To determine a_i, take the inner product projection (orthogonal projection) of Equation (2.8) onto the subspace F_n spanned by $\{\psi_i\}$ resulting in the following set of linear equations for the coefficients a_i.

$$\sum_{i=1}^{n} (L\varphi_i, \psi_j)\, a_i = (f, \psi_j) \qquad j = 1, 2, \ldots, n \qquad (2.9)$$

This can be put into matrix form,

$$[\mathcal{L}_{ji}]\,[a_i] = [g_j] \qquad (2.10)$$

where,

$$[\mathcal{L}_{ji}] = \begin{bmatrix} (L\varphi_1, \psi_1) & (L\varphi_2, \psi_1) & \cdots & (L\varphi_n, \psi_1) \\ (L\varphi_1, \psi_2) & (L\varphi_2, \psi_2) & \cdots & (L\varphi_n, \psi_2) \\ \cdots & \cdots & \cdots & \cdots \\ (L\varphi_1, \psi_n) & (L\varphi_2, \psi_n) & \cdots & (L\varphi_n, \psi_n) \end{bmatrix} \qquad (2.11)$$

$$[a_i] = \begin{bmatrix} a_1 \\ \cdot \\ \cdot \\ \cdot \\ a_n \end{bmatrix} \qquad (2.12)$$

$$[g_j] = \begin{bmatrix} (f, \psi_1) \\ \cdot \\ \cdot \\ \cdot \\ (f, \psi_n) \end{bmatrix} \qquad (2.13)$$

Having obtained the resulting coefficients a_i from (2.10), the unknown function e is determined by (2.7). This is the so-called "Galerkin-Petrov Method".

$\{\phi_i\}$ are called the expansion or basis functions, while $\{\psi_i\}$ are the testing or weighting functions. Since the accuracy of this method and the rate of convergence of the solution depend entirely upon the choice of both expansion and testing functions, some cases of particular interest are given next.

2.1.1 Method of Least Squares

Consider the residual norm,

$$\|Le_n - f\|^2 = \|Le_n\|^2 - 2< Le_n, f > + \|f\|^2 \tag{2.14}$$

Substitution of e_n by

$$e_n = \sum_{i=1}^{n} a_i \phi_i$$

we get

$$\|Le_n - f\|^2 = \sum_{i=1}^{n} \sum_{j=1}^{n} a_i a_j < L\phi_i, L\phi_j > - 2\sum_{i=1}^{n} a_i <L\phi_i, f > + \|f\|^2 \tag{2.15}$$

Equation (2.15) is then minimized

$$\frac{d}{da_k} \|Le_n - f\|^2 \tag{2.16}$$

to give

$$\sum_{i=1}^{n} (L\varphi_i, L\varphi_k)\, a_i = (L\varphi_k, f) \qquad k = 1, \ldots, n \tag{2.17}$$

From Equation (2.17) we conclude that if we choose

$$\psi_i = L\varphi_i \tag{2.18}$$

we get the best solution of the operator equation in the sense that an L_2 norm (root mean squares) is minimized. This is often called the method of least squares.

2.1.2 Bubnov-Galerkin Method

If we choose the subspaces E_n and F_n to be spanned by the same linearly independent functions, i.e.

$$\psi_i = \varphi_i \tag{2.19}$$

Equation (2.9) becomes,

$$\sum_{i=1}^{n} (L\varphi_i, \varphi_j)\, a_i = (f, \varphi_j) \qquad j = 1, 2, \ldots, n \tag{2.20}$$

Equation (2.20) has the advantage that if L is a symmetric operator, the matrix

$$\ell_{ij} = (L\varphi_i, \varphi_j) \tag{2.21}$$

will be a symmetric matrix.

The Bubnov-Galerkin approximation produces faster converging solutions with higher accuracy than the collocation method presented in the next section.

2.2 The Collocation Method

This is a projective method and it is also called "point matching".

Consider n sampling functions

$$\{w_i \mid_{i = 1, 2, \ldots, n}\}$$

linearly independent and spanning the subspace F_n. Each of these functions has a unity value at one of the sampling points and zero elsewhere. This means that the weighting functions are chosen to be the delta functions

$$w_i = \delta (x - x_i) \qquad (2.22)$$

where x_i are the sampling points.

Also, consider the subspace E_n spanned by n linearly independent basis functions,

$$\{\gamma_i \mid_{i = 1, 2, \ldots, n}\}$$

Here, the approximate solution of Equation (2.1)

$$e_n = \sum_{i=1}^{n} a_i \gamma_i$$

is determined by satisfying

$$L e_n = f \tag{2.23}$$

at the n sampling points in the region of interest.

2.3 The Method of Subsections

In this method, each of the basis functions exist only over subsections within the domain of e. The pulse function can be used over one subinterval. A linear combination of these pulses gives the step approximation to e.

A well behaved function is the triangle function. This is usually used over a group of adjacent subintervals. A piecewise linear approximation is obtained by a linear combination of these functions.

Sometimes, it is convenient to use the point mathcing method in conjunction with the subsectional method.

CHAPTER III

APPLICATION OF NUMERICAL TECHNIQUES TO WIRE ANTENNA AND SCATTERER PROBLEMS

3.1 Introduction

This chapter is devoted to presenting some numerical techniques useful for solving antenna problems. The problem of radiation and scattering by wire objects of arbitrary shape is solved in details using different methods. Also, the treatment of wire junctions is suggested here, with previous trials for solving it.

Generally speaking, the projection method has the advantages of flexibility and simplicity. Therefore, it can be used in the study of the electromagnetic behaviour of a single wire antenna, arrays of wire antennas and wire antennas of arbitrary orientation. In each case, the defining integral is replaced by a matrix equation and solved by matrix inversion to get the current. The structure of the antenna may be very complex, but the method does not change. Once the current distribution is obtained, the antenna behaviour can be easily determined.

3.2 Formulation of the Problem

The problem of finding the current distribution on wire antennas and scatterers is a particular case of the general boundary value problem involving

conducting bodies in a known impressed field, E^{im}. If the source is distant from the body it is viewed as a scatterer, and if the source is on the body it is considered an antenna. The boundary condition at the surface of each perfect conductor is,

$$\bar{n} \times \bar{E}^t = 0 \tag{3.1}$$

where,

$$\bar{E}^t = \bar{E}^{im} + \bar{E}^s \tag{3.2}$$

Substituting (3.2) into (3.1), the condition (3.1) results in

$$\bar{n} \times \bar{E}^s = -n \times \bar{E}^{im} \tag{3.3}$$

where

$\bar{n}$ is a unit vector normal to the surface of the conductor in the outward direction.

$\bar{E}^t$ is the total electric field vector consisting of both impressed field vector $\bar{E}^{im}$ and scattered field vector $\bar{E}^s$. The latter is defined as the field produced by the induced current on the conductors.

The basic equations that summarize this boundary value problem are,

$$\bar{E}^s = -jw\bar{A} - \bar{\nabla}\varphi \tag{3.4}$$

$$\bar{A} = \frac{\mu}{4\pi} \iint_S J \frac{e^{-jkR}}{R} dS \tag{3.5}$$

$$\varphi = \frac{1}{4\pi\epsilon} \oiint_S \sigma \frac{e^{-jkR}}{R} dS \qquad (3.6)$$

$$\sigma = -\frac{1}{jw} \nabla \cdot \bar{J} \qquad (3.7)$$

together with Lorentz's relation

$$\nabla \cdot A = -jw\epsilon\mu\varphi \qquad (3.8)$$

Here, $\bar{A}$, $\bar{J}$, σ, φ, μ and ϵ are used to denote the magnetic vector potential, the electric current density, the electric charge density, the scalar potential, the permeability and the permittivity respectively. R is the distance from the source point to the field point, and S is the surface of the conductor.

In the study of antenna theory, the knowledge of current distribution is of fundamental importance. Equations (3.3) through (3.8) are used to fomulate the integral equation for the current on the antenna. Mei [12] showed the ease of direct numerical calculation for the wire antenna integral equations usually encountered. These are the Integro-differential equation, Pocklington's equation and Hallen's equation.

3.3 Current Approximation

The solution of an integral equation for the current cannot be exactly determined. Several approximate methods for solving this equation are

used in the antenna theory. The approximate current distributions which are usually used in these methods should satisfy some practical requirements. The most important one is that it must be a good overall approximation along the antenna length to yield an accurate radiation pattern.

The sinusoidal current distribution along the cylindrical antennas was the first approximate current distribution used for solving the integral equation and analysing the radiation properties of such structures. Unfortunately, this type of approximation is quite inaccurate. Various correction terms, usually some other trigonometric functions, are added to the leading sinusoidal term. The modified current distributions agree much better with experimental results.

Another type of approximation is the expansion of the current into pulses resulting in a step approximation to the current [23] or its expansion into triangles resulting in a piecewise linear current approximation [2, 10]. The wire is divided into a number of short segments connected together. Each pulse extends over only one segment while each triangle extends over four adjacent segments.

Since the current distribution is a well behaved function, it can be approximated accurately by a polynomial of a relatively low order with complex coefficients [13, 14]

Lagrangian interpolation polynomials [18, 19] have been used to approximate the currents on a wire antenna structure. These polynomials are of theoretical and practical interests. Some details on this interesting kind of approximation will be given later.

3.4 Solution of Integro-Differential Equations by the Method of Subsections

Here, the integro-differential equation is solved using the method of subsections. In this method, the antenna structure is divided into a number of segments. Current expansion functions are taken to be nonzero over each segment or a group of adjacent segments and zero everywhere else.

For thin wires, the following approximations can be used:

1. The currents and charges are assumed to flow in the axial direction in a filamentary manner.

2. If a denotes the wire radius and ℓ its length and λ the wavelength, we have $a \ll \ell$ and $a \ll \lambda$.

3. All wire segments are assumed to be made of perfect conductors so that the boundary condition (3.3) can be applied.

Using these approximations, Equations (3.3) through (3.7) reduce to:

$$-E_z^i = -jw\bar{A} - \frac{\partial \varphi}{\partial z}\,\hat{\mu}_z \quad \text{on } S \tag{3.9}$$

$$\bar{A} = \frac{\mu}{4\pi} \int_{\text{axis}} \bar{I}(z)\, \frac{e^{-jkR}}{R}\, dz \tag{3.10}$$

$$\varphi = \frac{1}{4\pi\epsilon} \int_{\text{axis}} \sigma(z)\, \frac{e^{-jkR}}{R}\, dz \tag{3.11}$$

$$\sigma = -\frac{1}{jw}\,\frac{dI(z)}{dz} \tag{3.12}$$

where z is the length variable along the wire axis. The additional boundary condition $I = 0$ at the ends of each wire must also be satisfied. Substitution of (3.10) - (3.12) into (3.9) gives the integro-differential equation,

$$L(\bar{I}) = \bar{E}^{i}_{tan} \quad \text{on} \quad S \tag{3.13}$$

where the integro-differential operator L is given by

$$L(\bar{I}) = \left[jw\bar{A} + \frac{\partial \varphi}{\partial z} \right]_{tan} \tag{3.14}$$

It is interesting to note that Equation (3.13) has exactly the same form as (2.1). Therefore, making use of the method of moments [6,7], and using the approximation of the current $\bar{I}$ as,

$$\bar{I} = \sum_{i} \sum_{n} I_{i,n} \bar{F}_{i,n} \tag{3.15}$$

Equation (3.13) reduces to,

$$\sum_{i} \sum_{n} I_{in} L \bar{F}_{in} = \bar{E}^{i}_{tan} \tag{3.16}$$

where $\bar{F}_{in}$ is a set of expansion functions, and I_{in} are the complex coefficients to be determined. Taking the inner product of Equation (3.16) with each testing function W_{jm}, this results in

$$\sum_i \sum_n I_{in} \langle \overline{W}_{jm}, L\overline{F}_{in} \rangle = \langle W_{jm}, \overline{E}^i_{tan} \rangle \qquad (3.17)$$

$$j = 1, 2, \ldots, NW$$

$$m = 1, 2, \ldots, NE(j)$$

where NW is the number of wires and NE(j) is the number of ~~expansion~~ testing functions on the j^{th} wire.

Equation (3.17) can be written as a matrix equation,

$$[Z][I] = [V] \qquad (3.18)$$

[Z] is called the generalized impedance matrix, [V] the generalized voltage vector and [I] the generalized current vector. Therefore, the complex current coefficients are given by

$$[I] = [Y][V] \qquad (3.19)$$

where [Y] is called the generalized admittance matrix.

Strait and Hirasawa [23] used the subsectional point matching method with pulses as expansion functions. Kuo and Strait [10] and Chao and Strait [2, 3] used Galerkin's method with triangular current expansion functions. Harrington and Mautz [8] have solved the single straight wire problem using three different procedures. These include point matching with pulses as basis functions, point matching with triangle expansion functions, and Galerkin's procedure with triangle expansion functions. They found that, with segments less than $\lambda/10$ in

length, no significant difference in results is observed between the last two methods and that they converge about twice as fast as the first.

Subsectional piecewise sinusoidal functions [22] are used for both expansion and weighting functions resulting in a Galerkin solution to the analysis of wire problems. This is suggested by Richmond and programmed by Strait et al. The Near electric and magnetic fields of wire antennas [29] have been computed by Warren et al. They solve the resulting integro-differential equation using subsectional point matching methods with pulse current expansion functions.

3.5 Hallen's Equation and Polynomial Current Approximation

Popovic [T3] formulated the integral equation for the current on an isolated, symmetrical cylindrical dipole of length 2h. He considered a delta function generator of voltage V and used Equations (3.3) - (3.4) together with Lorentz condition (3.8) to get the differential equation for the vector potential A_z along the antenna whose axis coincides with the z-axis.

$$jw\left(1 + \frac{1}{k^2}\frac{\partial^2}{\partial z^2}\right) A_z = V\,\delta(z) \qquad (3.20)$$

The solution is found to be:

$$A_z = C_1 \cos kz + \frac{kV}{2jw} \sin k|z| \qquad (3.21)$$

Equating the right hand sides of Equations (3.5) and (3.21), we obtain the approximate form of the Hallen's integral equation for current along the dipole.

$$\int_{-h}^{h} I(z') \frac{e^{-jkR}}{R} dz' = C \cos kz + \frac{V}{j60} \sin k|z| \qquad (3.22)$$

where

$$C = 4\pi C_1/\mu_o$$

$$\frac{1}{j60} = 4\pi k/(2jw\mu_o)$$

$$R = \{(z-z')^2 + a^2\}^{1/2}$$

According to the method of undetermined coefficients, $I(z')$ is represented by a series of known functions with unknown complex coefficients. These coefficients are then determined by satisfying Equation (3.22) at as many points along the antenna as are needed to determine these coefficients.

It is assumed that $I(z')$ can be represented in the form of a polynomial of n^{th} order;

$$I(z') = \sum_{m=1}^{n} I_m (1 - |z'|/h)^m \qquad (3.23)$$

where I_m are the complex coefficients to be determined. With this current distribution function, Equation (3.22) becomes

$$\sum_{m=1}^{n} I_m \int_{-h}^{h} (1 - |z'|/h)^m \frac{e^{-jkR}}{R} dz' = C \cos kz + \frac{V}{j60} \sin k|z| \qquad (3.24)$$

Now, let Equation (3.24) be satisfied at the points

$$z_p, \qquad p = 1, 2, \ldots, (n+1)$$

This results in $(n+1)$ complex linear equations in $(n+1)$ complex unknowns $I_1, I_2, \ldots, I_n$ and C:

$$\sum_{m=1}^{n} I_m F_m(z_p) - C \cos k z_p = \frac{V}{j60} \sin k |z_p| \qquad p = 1, 2, \ldots, (n+1) \tag{3.25}$$

where,

$$F_m(z_p) = \int_{-h}^{h} (1 - |z'|/h)^m \frac{e^{-jkR_p}}{R_p} dz' \tag{3.26}$$

and

$$R_p = \{(z_p - z')^2 + a^2\}^{\frac{1}{2}}$$

The best choice of the z_p points is:

$$z_p = (p-1)\, h/n \qquad p = 1, 2, \ldots, (n+1) \tag{3.27}$$

Evaluating the integrals of (3.26) numerically, we can solve the system of linear Equations (3.25) for $I_1, I_2, \ldots, I_n$.

Popovic [14] used the same approach to get the current distributions on two identical parallel, arbitrarily located thin antennas. Two simultaneous

integral equations for currents $I_1(z)$ and $I_2(z)$ are obtained. Using the method of undetermined coefficients, these integral equations can be reduced to two sets of linear equations for the unknown parameters,

$$I_m^{(1)} \text{ and } I_m^{(2)}, \quad m = 1, 2, \ldots, n$$

3.6. Bubnov-Galerkin Projective Method for Antenna Problems

This method is intensively discussed and analysed by Silvester and Chan [18, 19]. They found that the most convenient equation to use is the Pocklington equation.

In this section, Poklington's equations for arbitrary configurations of straight wires are derived and then solved using the Galerkin projective method. Consider two wires m and n arbitrarily located in space, and of different lengths $2h_m$ and $2h_n$ respectively. The following derivation uses the approximation of making the source point (s_m) on the axis of wire m and the field point (s_n) on the surface of wire n. Using Equations (3.4) and (3.8), we get

$$\bar{E}(s_n) = -jw\bar{A} + \frac{1}{jw\epsilon\mu} \text{ grad div } \bar{A} \qquad (3.28)$$

where the magnetic vector potential is given by,

$$\bar{A}(s_n) = \frac{\mu}{4\pi} \int_{-h_m}^{h_m} \hat{m}\, I^m(s_m)\, \frac{\exp(-jkR_{mn})}{R_{mn}}\, ds_m \qquad (3.29)$$

The electric field components of Equation (3.28) in cylindrical coordinates are,

$$E_z = -jwA_z + \frac{1}{jw\mu\epsilon} \frac{\partial}{\partial z} \left(\frac{\partial A_z}{\partial z} \right) \tag{3.30}$$

$$E_\rho = \frac{1}{jw\mu\epsilon} \frac{\partial}{\partial \rho} \left(\frac{\partial A_z}{\partial z} \right) \tag{3.31}$$

$$E_\varphi = 0 \tag{3.32}$$

Carrying out the differentiations by using (3.29), Equations (3.30) and (3.31) are reduced to

$$E_z = \int_{-h_m}^{h_m} I^m(s_m) \frac{\exp(-jkR_{mn})}{jw\epsilon\, 4\pi R_{mn}^5} \left[2R_{mn}^2 (1 + jkR_{mn}) - (\rho^2 + a_n^2) \cdot (3 + j3kR_{mn} - k^2 R_{mn}^2) \right] ds_m \tag{3.33}$$

$$E_\rho = \int_{-h_m}^{h_m} I^m(s_m) \frac{\exp(-jkR_{mn})}{jw\epsilon\, 4\pi R_{mn}^5} \left[\rho(z - s_m)(3 + j3kR_{mn} - k^2 R_{mn}^2 \right] ds_m \tag{3.34}$$

Substitute (3.33) and (3.34) into

$$\bar{E}(s_n) = \hat{\rho} E_\rho + \hat{z} E_z \tag{3.35}$$

and then take the dot product of the resulting equation with $\hat{n}$, the tangential electric field $E^{tan}_{nm}(s_n)$ on the surface of element n due to element m is given by

$$E^{tan}_{nm}(s_n) = \frac{1}{j\omega\epsilon\, 4\pi} \int_{-h_m}^{h_m} I^m(s_m)\, F(s_n, s_m)\, ds_m \tag{3.36}$$

where $I^m(s_m)$ is the current on element m, and

$$F(s_n, s_m) = \frac{\exp(-jkR_{mn})}{R^5_{mn}} \left[\hat{m}\cdot\hat{n}\, R^2_{mn}\,(-1 - jkR_{mn} + k^2R^2_{mn}) + (R_{mn}\cdot\hat{m})(R_{mn}\cdot\hat{n})(3 + j3kR_{mn} - k^2R^2_{mn})\right] \tag{3.37}$$

$$R^2_{mn} = (x_n - x_m + s_n\,\hat{x}\cdot\hat{n} - s_m\,\hat{x}\cdot\hat{m})^2 + (y_n - y_m + s_n\,\hat{y}\cdot\hat{n} - s_m\,\hat{y}\cdot\hat{m})^2 + (z_n - z_m + s_n\,\hat{z}\cdot\hat{n} - s_m\,\hat{z}\cdot\hat{m})^2 + a_n^2 \tag{3.38}$$

(x_n, y_n, z_n) and (x_m, y_m, z_m) are the cartesian coordinates of the centres of elements n and m respectively, $\hat{m}$ and $\hat{n}$ denote unit vectors directed along the axis of m and n respectively, a_n is the radius of element n. To apply

the boundary condition, we can use Equation (3.3) on the wire surface at s_n. Using Equation (3.36) and considering N wire elements the Pocklington's equations can be obtained.

$$\sum_{m=1}^{N} \frac{1}{j\omega\epsilon 4\pi} \int_{-h_m}^{h_m} I^m(s_m)\, F(s_n, s_m)\, ds_m + \hat{n} \cdot E_n^{im}(s_n) = 0 \,, \qquad n = 1, 2, \ldots, N \tag{3.39}$$

If we approximate the current in (3.39) by the finite set of linearly independent basis functions

$$I^m(s_m) = \Sigma\, I_\ell^m\, f_\ell(s_m) \tag{3.40}$$

Equation (3.39) becomes

$$\frac{1}{4\pi} \sum_{m=1}^{N} \sum_{\ell=1}^{L} \int_{-h_m}^{h_m} I_\ell^m\, f_\ell(s_m)\, F(s_n, s_m)\, ds_m = -j\omega\epsilon\, \hat{n} \cdot E_n^{im}(s_n) \qquad n = 1, 2, \ldots, N \tag{3.41}$$

where I_ℓ^m are the unknown complex coefficients to be determined.

Using the inner product projection of both sides of (3.41), onto the subspace spanned by the basis functions, Equation (3.41) results in

$$\frac{j\eta}{4\pi k} \sum_{m=1}^{N} \sum_{\ell=1}^{L} I_\ell^m \left[\int_{-h_n}^{h_n} f_i(s_n) \int_{-h_m}^{h_m} f_\ell(s_m)\, F(s_n, s_m)\, ds_m\, ds_n \right]$$

$$= \int_{-h_n}^{h_n} \hat{n} \cdot \bar{E}_n^{im}(s_n)\, f_i(s_n)\, ds_n$$

$$i = 1, 2, \ldots, L$$

$$n = 1, 2, \ldots, N \qquad (3.42)$$

Equation (3.43) can be put in the matrix form

$$[Z_{i',\ell'}][I_{\ell'}] = [V_{i'}] \qquad (3.43)$$

where $i' = i + (n-1)L$, $\ell' = \ell + (m-1)L$, $[Z]$, $[I]$ and $[V]$ have the same meaning as in Section 3.4. Therefore, the Bubnov-Galerkin solution is given by

$$[I_{\ell'}] = [Y_{i',\ell'}][V_{i'}] \qquad (3.44)$$

where $[Y]$ is the generalized admittance matrix.

3.7 Treatment of Wire Junctions

Using triangle expansion functions, Chao and Strait [2] showed that a junction of N wires can be treated as a problem involving N open ended wires with N - 1 overlaps. Hence, N - 1 triangle expansion functions overlap the junction. This treatment has been used in successful studies of several radiation and scattering problems [27].

Of course, junction problems can also be handled with other sets of expansion functions including pulses. Sayre [17] expanded the current in terms of pulse expansion functions properly positioned on the wire object such that the current is forced to zero at the wire ends. In the vicinity of a junction, the pulse expansions for the current on each wire are positioned such that each pulse ends at the junction. The continuity equation in its integral form is considered near the junction. It relates the total junction current to the charges on the wire segments forming the current.

Butler [2] established Hallen's integral equations for the skew crossed wires and used the method of moments to solve them. The complex unknown coefficients of the current are reduced by equating the currents to zero at the ends of the wires. An auxiliary equation, in terms of the unknown coefficients is obtained by equating the sum of the currents at the junction to zero. Solution of the algebraic equations results in the determination of the current coefficients.

Practically, the use of the method proposed by Chao and Strait is somewhat inconvenient. It requires that near the junction of N wires, overlaps of two segments must be included for (N - 1) of the wires in the geometry inputted to the program. Sayre's method using pulses is a low converging one with respect to other methods. The method of handling wire junctions proposed by Butler is restricted to skew crossed wires only.

However, a simple and general method to deal with wire junctions, presented by Silvester and Chan [19], will be discussed later.

This was a brief review of the various numerical methods that have been employed in the solution of wire antenna and scatterer problems. Methods for handling wire junctions were also included. The impressed field was considered arbi arbitrary, hence, both radiation and scattering problems can be solved.

CHAPTER IV

SOLUTION OF THE INTERCONNECTED STRAIGHT WIRE PROBLEM BY NEW TRANSFORMATION TECHNIQUES

This chapter is designed to provide the complete detailed analysis for solving any wire antenna or scatterer structure.

The main purpose is to follow some new transformations to get the current distributions on the wires of a scatterer structure. With these new treatments, difficult problems that have never been solved before, are easily analysed throught this chapter. The same approach can be used with wire antennas.

4.1 Formulation of the Self and Mutual Impedances of Two Arbitrarily Located Straight Thin Wires

Consider two straight wire elements m and n, having radii a_m and a_n and lengths S_m and S_n respectively, arbitrarily located in space, as shown in Figure 4.1.

Let these wire lengths and radii be such that $S_m/a \gg 1$, $S_n/a \gg 1$, $a_m \ll \lambda$ and $a_n \ll \lambda$, where λ is the wavelength. $\hat{m}$ and $\hat{n}$ are unit vectors directed along the axes, and giving the direction of current flow of m and n respectively. Consider two elements ds_m and ds_n on m and n at distances s_m and s_n from (x_m, y_m, z_m) and (x_n, y_n, z_n) respectively. ds_m is the element where the point source is located and ds_n is the element where the field point is

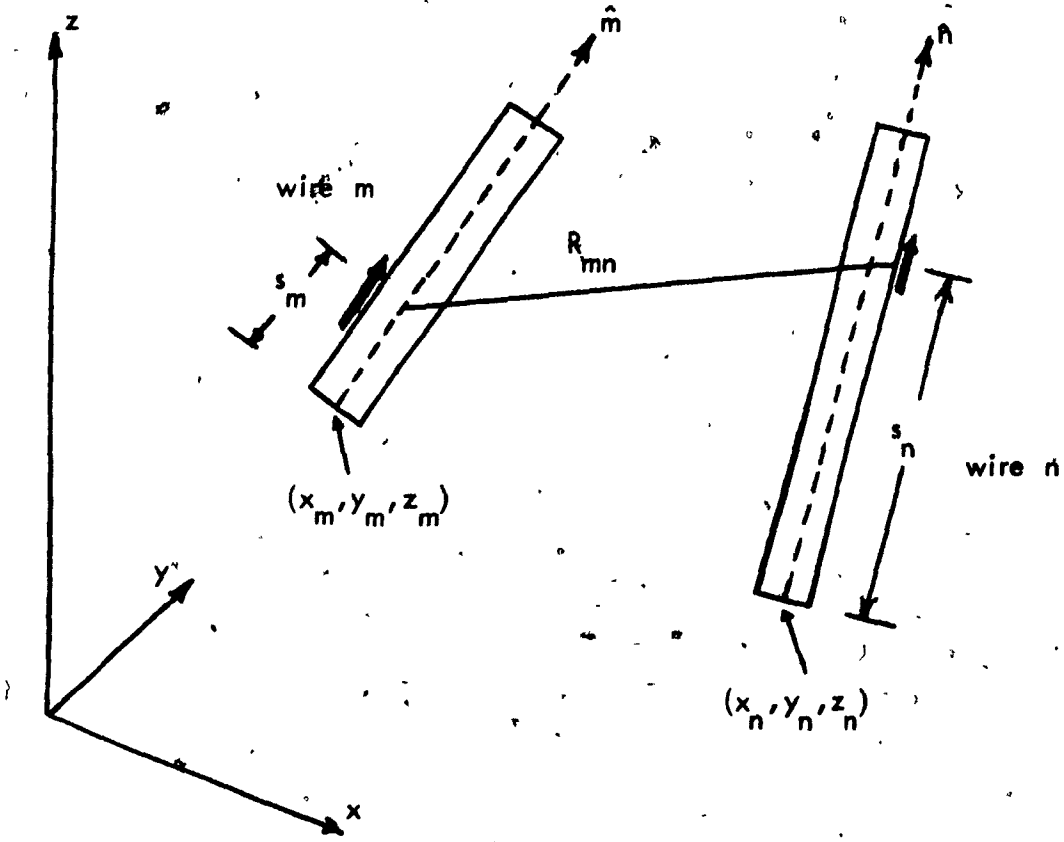

FIGURE 4.1 Two Arbitrarily Located Wires.

located.

The tangential electric field on the surface of element n due to a current $I^m(s_m)$ flowing on the axis of element m is given by Equation (3.37).

$$E^{tan}_{nm}(s_n) = \frac{1}{j\omega\epsilon 4\pi} \int_0^{S_m} F(s_n, s_m)\, I^m(s_m)\, ds_m \tag{4.1}$$

where,

$$F(s_n, s_m) = \frac{1}{R^5_{mn}} \exp(-jkR_{mn}) \left[\hat{m}\cdot\hat{n}\, R^2_{mn}(-1 - jkR_{mn} + k^2R^2_{mn}) \right.$$

$$\left. + (\bar{R}_{mn}\cdot\hat{m})(3 + 3jkR_{mn} - k^2R^2_{mn})(R_{mn}\cdot\hat{n})\right] \tag{4.2}$$

and

$$R^2_{mn} = (x_n - x_m + s_n\hat{x}\cdot\hat{n} - s_m\hat{x}\cdot\hat{m})^2 + (y_n - y_m + s_n\hat{y}\cdot\hat{n} - s_m\hat{y}\cdot\hat{m})^2$$

$$+ (z_n - z_m + s_n\hat{z}\cdot\hat{n} - s_m\hat{z}\cdot\hat{m})^2 + a^2_n \tag{4.3}$$

k = wave number

ϵ = permittivity of the medium

R_{mn} = distance between the field point on the wire surface and the source point on the wire axis.

The mutual impedance (referred to currents I^m_{max} and I^n_{max}) between the two wire elements m and n of Figure 4.1, can be determined by the well known induced emf method.

$$Z_{nm} = \frac{-1}{|I^m_{max}|\,|I^n_{max}|} \int_0^{S_n} E^{tan}_{nm}(s_n)\, I^{n*}(s_n)\, ds_n \qquad (4.4)$$

where

$I^n(s_n)$ = induced current on element n

$|I^m_{max}|$ and $|I^n_{max}|$ are the magnitudes of the maximum currents on elements m and n respectively.

By substituting Equation (4.1) into (4.4) we get

$$Z_{nm} = \frac{-1}{j\omega\epsilon 4\pi\,|I^m_{max}|\,|I^n_{max}|} \int_0^{S_m}\int_0^{S_n} F(s_n, s_m)\, I^m(s_m) I^n(s_n)\, ds_n\, ds_m \qquad (4.5)$$

Approximate each of the unknown currents $I^m(s_m)$ and $I^n(s_n)$ by a finite set of linearly independent interpolative basis functions in the form,

$$I^m(s_m) = \sum_{m=1}^{M} a_m f_m(s_m)$$

$$I^n(s_n) = \sum_{n=1}^{N} b_n f_n(s_n)$$

where

M and N are number of interpolation nodes for wires m and n,

f_m and $\mathcal{L}_n$ are polynomials,

a_m and b_n are the complex current coefficients to be determined.

Therefore, Equation (4.5) can be written as follows

$$Z_{nm} = \frac{-1}{j\omega\epsilon 4\pi |I^m_{max}| |I^n_{max}|} \sum_{m=1}^{M} \sum_{n=1}^{N} a_m \left(\int_0^{S_m} \int_0^{S_n} F(s_n, s_m) \right.$$

$$\left. f_m(s_m)\, \mathcal{L}_n(s_n)\, ds_n\, ds_m \right) b_n^* \qquad (4.6)$$

If we define the column vectors

$$A = \begin{bmatrix} a_1 \\ \vdots \\ a_M \end{bmatrix} \quad \text{and}$$

$$B = \begin{bmatrix} b_1 \\ \vdots \\ b_N \end{bmatrix} \quad \text{and}$$

the matrix P whose elements are

$$P_{mn} = \int_0^{S_m} \int_0^{S_n} F(s_n, s_m)\, f_m(s_m)\, f_n(s_n)\, ds_n\, ds_m \qquad (4.7)$$

the mutual impedance of Equation (4.6) can be put in matrix form

$$Z_{nm} = \frac{-1}{jw\epsilon 4\pi |I^m_{max}|\, |I^n_{max}|} A^T P B^* \qquad (4.8)$$

The self impedance Z_{mm} of element m should be equal to the mutual impedance Z_{nm} between n and m when $n = m$, and $f_n(s_n) = f_m(s_m)$, and when the kernel (4.2) of the matrix element P_{mn} reduces to [19]

$$F(s_m, s_n) = \frac{\exp(-jkR_{mn})}{R^5_{mm}} \left[(1 + jkR_{mm})(2R^2_{mm} - 3a^2_m) + k^2 a^2_m R^2_{mm}\right] \qquad (4.9)$$

where

$$R^2_{mm} = (s'_m - s_m)^2 + a^2_m \qquad (4.10)$$

Therefore, the self impedance can be written as

$$Z_{nm} = \frac{-1}{jw\epsilon 4\pi |I^m_{max}|^2} A^T P A^* \qquad (4.11)$$

It is clear that the entries P_{mn} to P in Equations (4.8) and (4.11) are exactly the same matrix elements of Z in Equation (3.43). Determination of

these entries is discussed in the next section. It is also clear that the components of vectors A and B in (4.8) and (4.11) are similar to that of the unknown vector [I] in (3.44).

Therefore, the determination of the complex current coefficients and hence the self and mutual impedances requires the solution of the system (3.44).

4.2 Determination of Matrix Elements

From section 4.1, we conclude that the determination of the self and mutual impedances depends entirely upon the entries P_{mn} to the matrix P. Therefore, evaluation of these matrix elements is needed. There are several possible situations to be examined independently.

4.2.1 Source and Field Points on Separate Wires

When the source point and the field point are on separate wires, as shown in Figure 4.1, $F(s_n, s_m)$ given by Equation (4.2) is continuous and finite everywhere. Since the integrand of (4.7) is smooth, the double integral can easily be evaluated numerically by double Gauss-Legendre quadrature formulae in the $s_n - s_m$ plane [9,24].

$$P_{mn} = \int_0^{S_n} \int_0^{S_m} K(s_n, s_m)\, ds_m\, ds_n$$

This could be evaluated to give

$$P_{mn} = \sum_{i=1}^{I} \sum_{j=1}^{J} W_i W_j K(s_{ni}, s_{mj}) \qquad (4.12)$$

where I, J are number of quadrature nodes to perform the integrations with respect to s_n and s_m respectively, and

$$K(s_n, s_m) = F(s_n, s_m) f_m(s_m) f_n(s_n) \qquad (4.13)$$

The number of quadrature nodes required depends on the degree of the current approximating polynomials as well as the distance between the wire elements. For example, at large distances, the integrand is smooth, hence fewer quadrature nodes are needed.

4.2.2 Source and Field Points on the Same Wires

When the source point and the field point are on the same wire, as shown in Figure 4.2 (a), $F(s_n, s_m)$ is given by Equation (4.9) and R_{mm} by (4.10). Here, the integrand is finite but varies very rapidly as s_m approaches s'_m, where R_{mm} becomes equal to the wire radius a_m. This wire radius is assumed to be very small.

By using similar transformations to those given by Silvester and Chan [18],

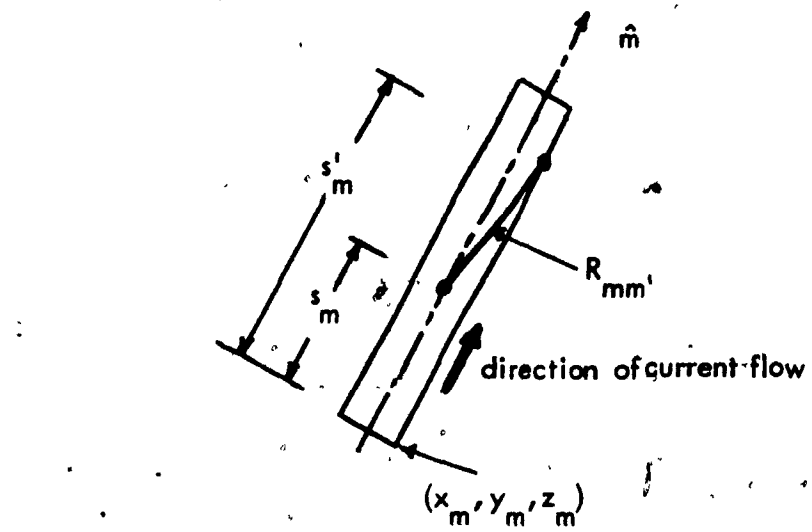

(a)

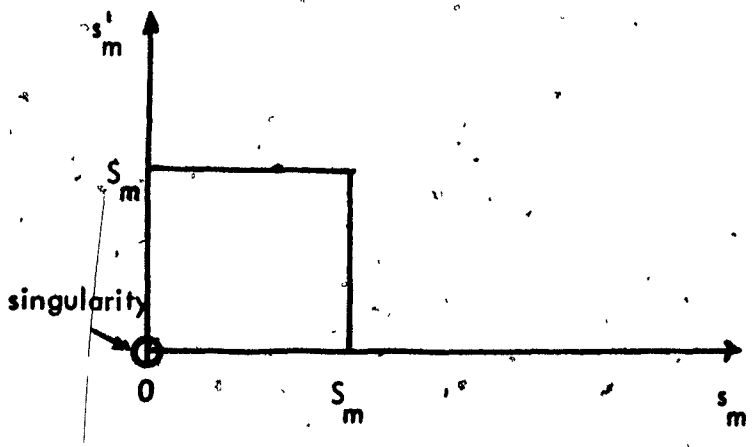

(b)

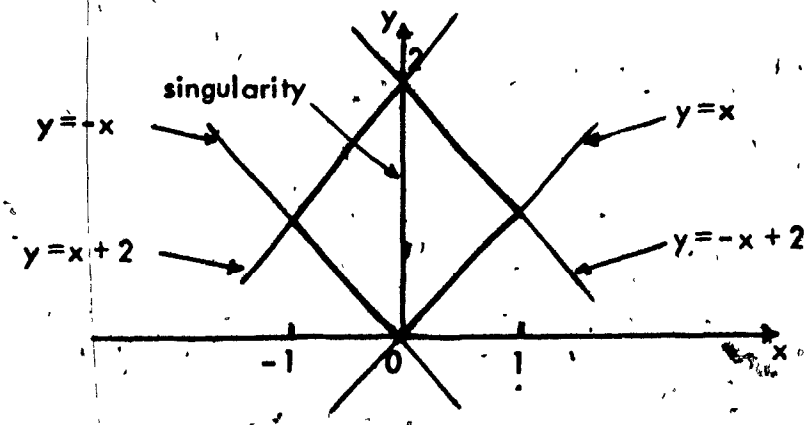

(c)

FIGURE 4.2 Transformation from $(s'_m - s_m)$ Plane to $(x-y)$ Plane, used for Single Wire Problems.

$$x = (s'_m - s_m)/S_m$$

$$y = (s'_m + s_m)/S_m \qquad (4.14)$$

together with

$$dx\,dy = \frac{2}{S_m^2}\, ds_m\, ds'_m$$

Equation (4.10) becomes

$$R_{mm}^2 = x^2 S_m^2 + a_m^2 \qquad (4.15)$$

This transfomation is illustrated in Figures 4.2(b) and 4.2(c).

Equation (4.7) then becomes

$$P_{mn} = \int_{-1}^{0} \frac{\exp(-jk S_m R)}{S_m^5 R^5} [(1+jk S_m R)(2 S_m^2 R^2 - 3 a^2) + k^2 S_m^2 R^2 a^2] \int_{-x}^{2+x} f_m((x+y)\frac{S_m}{2}) f_n((y-x)\frac{S_m}{2}) \frac{S_m^2}{2}\, dy\, dx$$

$$+ \int_{0}^{1} \frac{\exp(-jk S_m R)}{S_m^5 R^5} [(1+jk S_m R)(2 S_m^2 R^2 - 3 a^2) + k^2 S_m^2 R^2 a^2] \int_{x}^{2-x} f_m((x+y)\frac{S_m}{2}) f_n((y-x)\frac{S_m}{2}) \frac{S_m^2}{2}\, dy\, dx \qquad (4.16)$$

where

$$R^2 = x^2 + (a_m/S_m)^2 = R_{mm}^2/S_m^2 \qquad (4.17)$$

Put $x' = -x$ in the second integral of the first term in (4.16). Equation (4.16) reduces to

$$P_{mn} = \int_0^1 \frac{1}{S_m^5 R^5} \exp(-jk S_m R)\,[(1+jk S_m R)(2 S_m^2 R^2 - 3 a_m^2) + k^2 S_m^2 R^2 a^2]$$

$$\int_{x}^{2-x} [f_m((y-x)\frac{S_m}{2})\, f_n((y+x)\frac{S_m}{2}) + f_m((x+y)\frac{S_m}{2})\, f_n((y-x)\frac{S_m}{2})]$$

$$\frac{S_m^2}{2}\, dy\, dx \qquad (4.18)$$

Substituting $z = \frac{y-1}{1-x}$ and $dx\, dz = \frac{1}{1-x}\, dx\, dy$ in Equation (4.18) results in

$$P_{mn} = \frac{1}{2S_m} \int_0^1 \frac{\exp(-jk S_m R)}{R^5} [(1+jk S_m R)(2R^2 - 3\frac{a^2}{S_m^2}) + k^2 R^2 a^2]$$

$$(1-x) \int_{-1}^{1} [f_m\{(y(1-x)+1-x)\frac{S_m}{2}\}\, f_n\{(y(1-x)+1+x)\frac{S_m}{2}\}$$

$$+ f_m\{(y(1-x)+1+x)\frac{S_m}{2}\}\, f_n\{(y(1-x)+1-x)\frac{S_m}{2}\}]\, dy\, dx \qquad (4.19)$$

With these transformations, the kernel in the final Equation (4.19) is independent of y and is only a function of x. This kernel is nearly singular when x equals zero, while it is smooth for all values of y at a given x. Integration with respect to y is carried out using Gauss-Legendre quadratures. Integration with respect to x is evaluated using Gauss-Christoffel formula [4], with weight function $[x^2 + (\frac{a_m}{s_m})^2]^{-5/2}$, specially constructed for the purpose.

4.2.3 Source and Field Points on Two Connected Wires

The difficulty usually encountered by antenna engineers is the solution of the two connected wires problem, especially if these wires form very small angles. This problem has been solved by many of them [1,2,3,17], but it was restricted to a certain angle or a small range of angles. Chan [5] suggested an elegant approach to solve the wires at a junction. Unfortunately, this approach is inaccurate when the wires are unequal in lengths and radii. It can be more efficient, only when wires of equal lengths and radii are used. This restriction together with the small range of angles that can be treated, limit the usefulness of this approach.

Here, a new method for treating this problem, with wires forming any angle--whatever it could be--is carefully discussed and analysed. This method is general in the sense that it can analyse the problem when two wires of different radii and different lengths are joined at any angle.

Consider two wires m and n connected at one end and forming an angle θ. At this end the two coordinates (x_m, y_m, z_m) and (x_n, y_n, z_n)

are equivalent. The wire radii are a_m, a_n and lengths S_m and S_n respectively. $\hat{m}$ and $\hat{n}$ denote unit vectors directed along the axes of m and n, and give the reference directions of current flow. Also, consider two elements ds_m and ds_n on m and n at distances s_m and s_n, from the junction respectively.

Referring to Figure 4.3(a), the arrows give the reference directions of current flow. The distance R_{mn} between the field point s_n and the source point s_m is given by

$$R_{mn}^2 = (s_m^2 + s_n^2 - 2 s_m s_n \cos\theta + a_n^2) \tag{4.20}$$

The integrals of Equations (4.7) have a near singularity when both s_m and s_n approach the junction point. It is possible to rewrite expression (4.7) using the following transformation so as to simplify the integrations considerably. Set

$$\begin{bmatrix} x \\ y \end{bmatrix} = \begin{bmatrix} \sin\frac{\theta}{2} & \sin\frac{\theta}{2} \\ \cos\frac{\theta}{2} & -\cos\frac{\theta}{2} \end{bmatrix} \begin{bmatrix} s_n \\ s_m \end{bmatrix} \tag{4.21}$$

with this transformation, Equation (4.20) becomes

$$R_{mn}^2 = x^2 + y^2 + a_m^2 \tag{4.22}$$

and the elementary area in the x-y plane is,

$$dx\, dy = \sin\theta\, ds_n\, ds_m \tag{4.23}$$

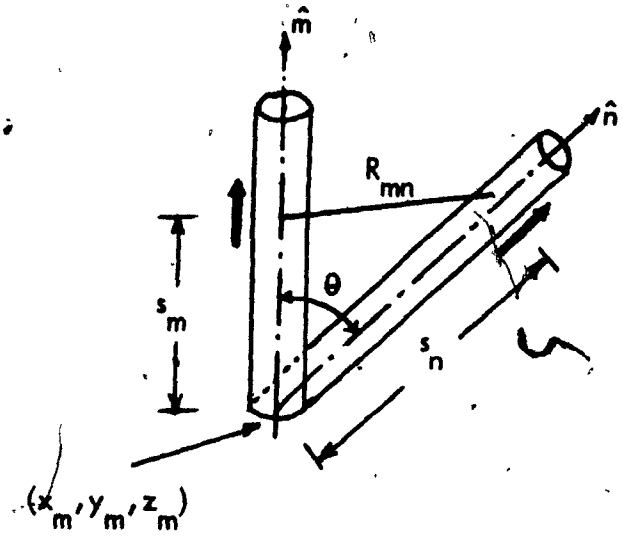

(a)

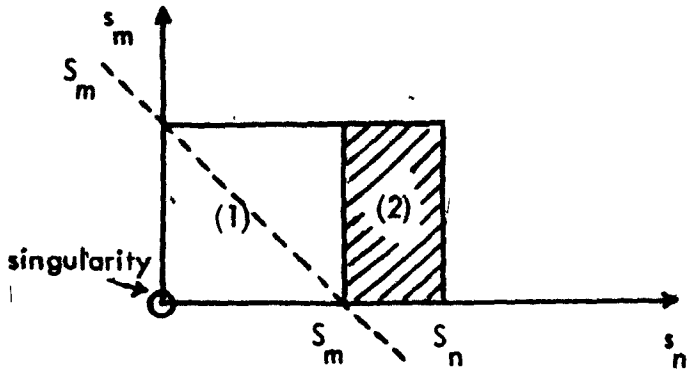

(b)

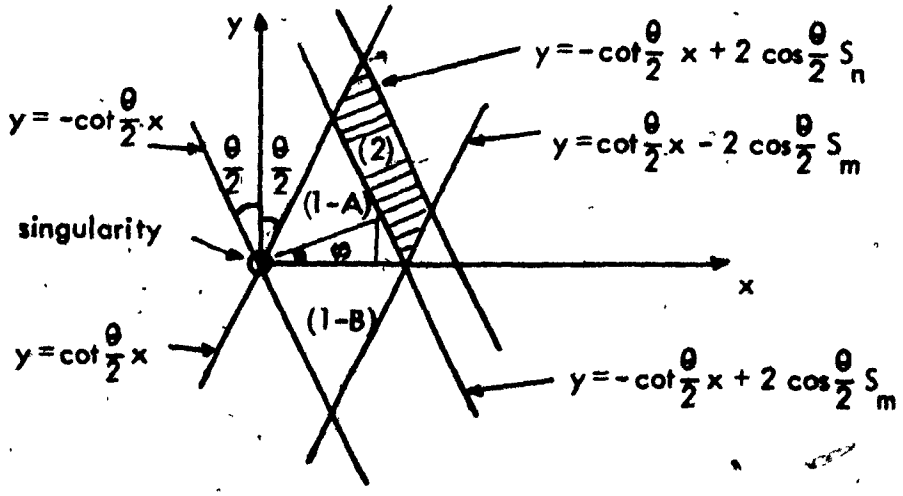

(c)

FIGURE 4.3 Transformation from $(s_m - s_n)$ Plane to $(x - y)$ Plane, used for the Two Connected Wire Problem of (a).

and the limits of integration in $s_m - s_n$ and x-y planes are shown in Figures 4.4(b), 4.4(c).

Numerical integration is the range $S_m \leq s_n \leq S_n$, the shaded area in Figures 4.4(b), 4.4(c), should be easy since the integrand is smooth and the kernel function is continuous. A cartesian product of Gauss-Legendre quadrature formulae can be used here.

$$P_{mn2} = \int_{S_m}^{S_n} \int_{0}^{S_m} K(s_n, s_m)\, ds_m\, ds_n \tag{4.24}$$

this could be written as

$$P_{mn2} = \sum_{i=1}^{I} \sum_{j=1}^{J} W_i W_j K(s_{ni}, s_{mj}) \tag{4.25}$$

where I, J are numbers of quadrature nodes required to perform the integration in s_n and s_m directions respectively. $K(s_n, s_m)$ is given by (4.13).

The troublesome region, region 1 in Figure 4.4(b), occurs in the vicinity of the singularity. In this area, P_{mn} can be written as

$$P_{mn1} = \int_{0}^{S_m} \int_{0}^{S_m} \frac{1}{R_{mn}^5} g(s_n, s_m)\, ds_n\, ds_m \tag{4.26}$$

where

$$g(s_n, s_m) = R_{mn}^5 K(s_n, s_m) \tag{4.27}$$

Divide this region of integration into (1-A) and (1-B) and use the transformation,

$$x = r \cos\varphi$$
$$y = r \sin\varphi \qquad (4.28)$$

together with

$$dx\, dy = r\, dr\, d\varphi \qquad (4.29)$$

Combining (4.21) and (4.28), the complete transformation of coordinates becomes

$$s_n = \frac{r}{2} \operatorname{cosec}\frac{\theta}{2} \cos\varphi + \frac{r}{2} \sec\frac{\theta}{2} \sin\varphi$$
$$s_m = \frac{r}{2} \operatorname{cosec}\frac{\theta}{2} \cos\varphi - \frac{r}{2} \sec\frac{\theta}{2} \sin\varphi \qquad (4.30)$$

and Equation (4.22) reduces to

$$R_{mn}^2 = r^2 + a_n^2 \qquad (4.31)$$

To find the limits, region 1-A is bounded by $\varphi = 0$, $\varphi = (\pi - \theta)/2$ and

$$y = -\cot\frac{\theta}{2}\, x + 2 \cos\frac{\theta}{2}\, S_m \qquad (4.32)$$

or

$$r_o \sin\varphi = -\cot\frac{\theta}{2}(r_o \cos\varphi) + 2 \cos\frac{\theta}{2}\, S_m \qquad (4.33)$$

giving

$$r_o = \frac{S_m \sin\theta}{\cos\left(\varphi - \frac{\theta}{2}\right)} \tag{4.34}$$

Using (4.23), (4.29) through (4.31) and Equation (4.34), Equation (4.26) yields,

$$P_{mn1} = \frac{1}{\sin\theta} \int_{\varphi=0}^{\frac{\pi-\theta}{2}} d\varphi \int_{r=0}^{r_o} \frac{1}{(r^2 + a_n^2)^{5/2}} \tag{4.35}$$

$$[g(r,\varphi) + g(r,-\varphi)]\, r\, dr$$

Again, if we consider the following transformation,

$$r = r_o z \tag{4.36}$$

$$dr = r_o dz \tag{4.37}$$

Equation (4.35) becomes

$$P_{mn1} = \frac{1}{\sin\theta} \int_{\varphi=0}^{\frac{\pi-\theta}{2}} d\varphi \int_{z=0}^{1} \frac{1}{\left(z^2 + \frac{a_n^2}{r_o^2}\right)^{5/2}} \tag{4.38}$$

$$[g(r_o z,\varphi) + g(r_o z,-\varphi)]\, \frac{1}{3}\, r_o\, z\, dz$$

The integration with respect to φ now involves an integrand bounded and continuous throughout the region of integration. Thus, it can be carried out using Gauss-Legendre quadrature formula. The integration with respect to z, whose weight function depends on r_o and hence on φ, varies very rapidly near $z = 0$. A Guass-Christoffel quadrature formula with weight function

$$(z^2 + \frac{a_n^2}{2r_o})^{-5/2}$$

is used.

This approach requires generation of as many special quadrature formulae as there are nodes in the φ direction. Since this number might be of the order of 4, no fundamental difficulty arises.

For more general solutions, two other cases have to be considered according to the directions of current flow. The transformations used before are exactly the same, but the singularities appear at different positions in the $s_m - s_n$ plane. These are illustrated in Figures 4.4 and 4.5.

4.2.4 Source and Field Points on Two Collinear Wires

This case is usually encountered in practice, especially in multi-dimensional wire structures. A vertical wire in the presence of an infinite ground plane could also be analysed as two collinear wires. This type of problem has been solved by many research workers in this area. The most interesting solution is that of Chan [5]. Again, his method in the special case of two collinear wires, is restricted

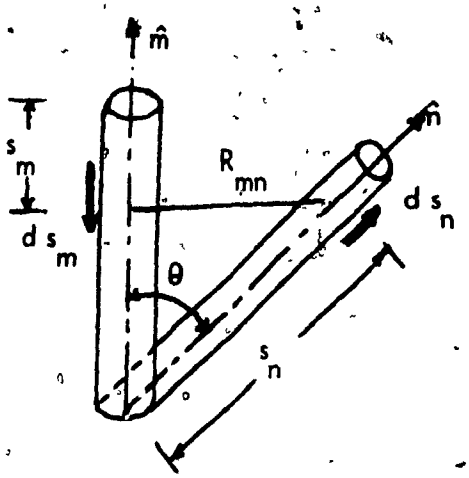

(a)

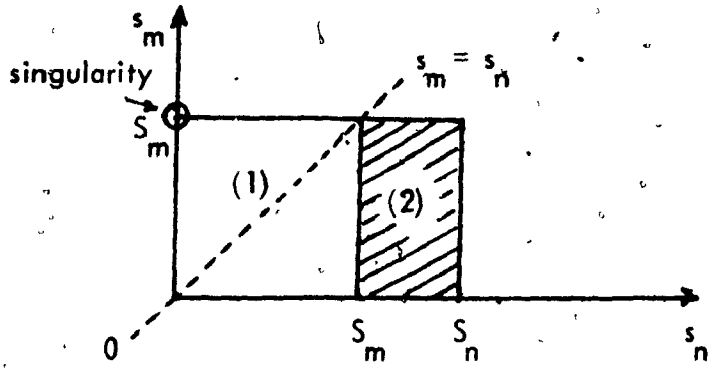

(b)

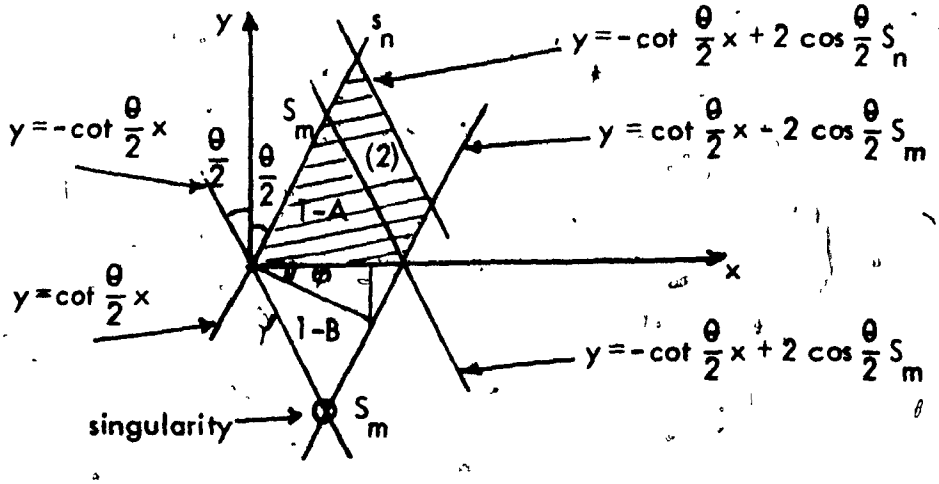

(c)

FIGURE 4.4 Transformation from $(s_m - s_n)$ Plane to $(x-y)$ Plane, used for the Two Connected Wire Problem of (a).

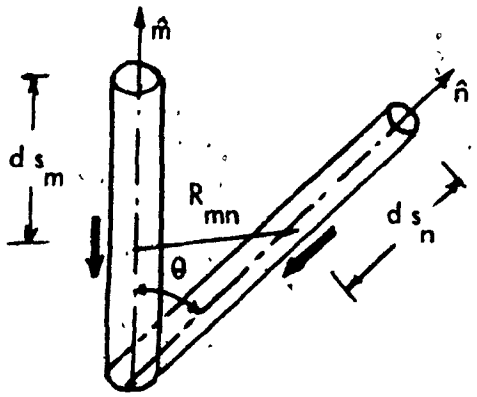

(a)

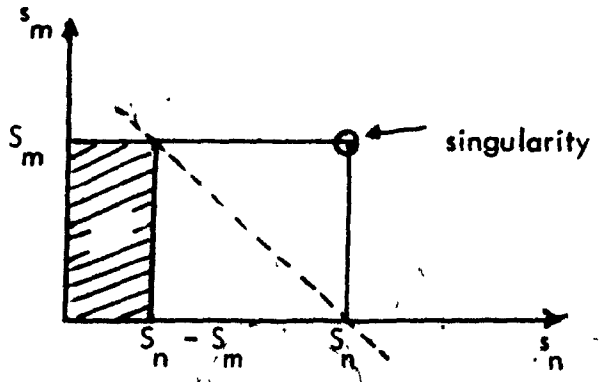

(b)

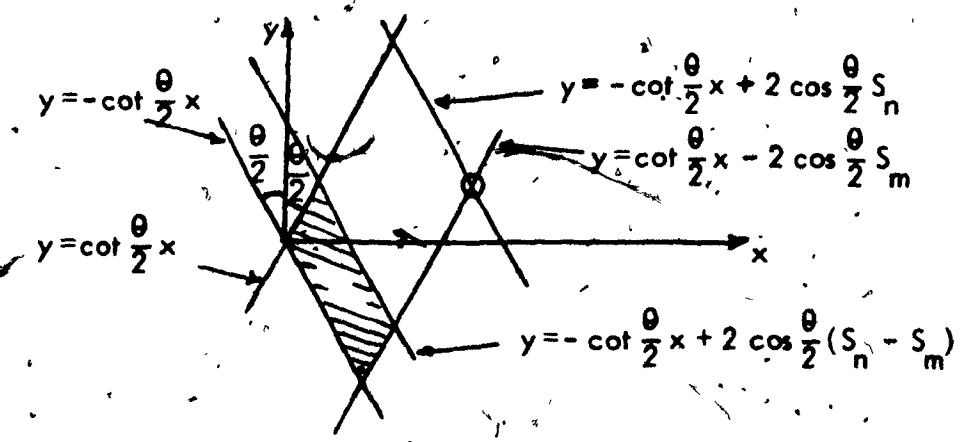

(c)

FIGURE 4.5 Transformation from $(s_m - s_n)$ Plane to $(x-y)$ Plane used for the Two Connected Wire Problem of (a).

to equal lengths and radii.

A general and elegant approach to solve this type of wire structure is presented here. This is general in the sense that collinear wires of unequal radii and lengths can be efficiently analysed.

Consider Figure 4.6(a) where the two wires n and m are collinear of unequal lengths S_m and S_n and radii a_m and a_n. The currents, in opposite directions are directed towards the free ends. R_{mn} is the distance between the source point s_m and the field point s_n.

$$R_{mn}^2 = (s_n + s_m)^2 + a_n^2 \tag{4.39}$$

Area (2) of Figure 4.6(b) has a smooth integrand. Gauss-Legendre formulae in both s_n and s_m directions are used.

The singularity of (4.7) appears when both s_n and s_m are equal to zero. The following transformation is used to shift the singularity in only one direction, as shown in Figure 4.6(c).

Using

$$u = (s_n + s_m)/S_m$$

$$v = (s_n - s_m)/S_m \tag{4.40}$$

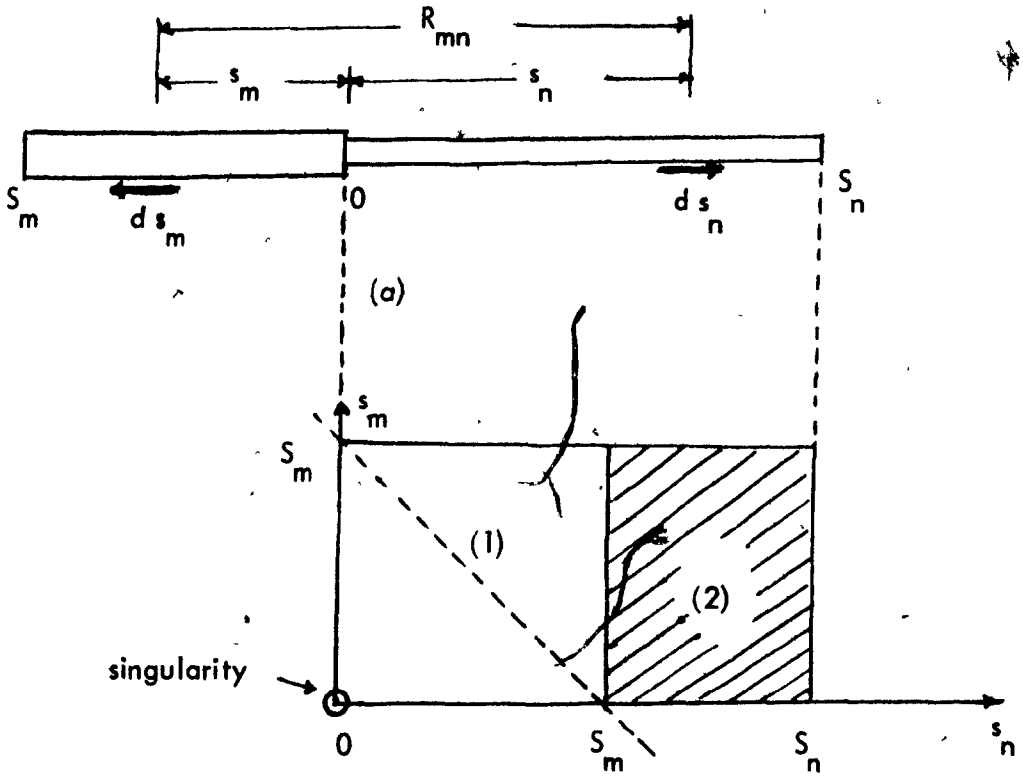

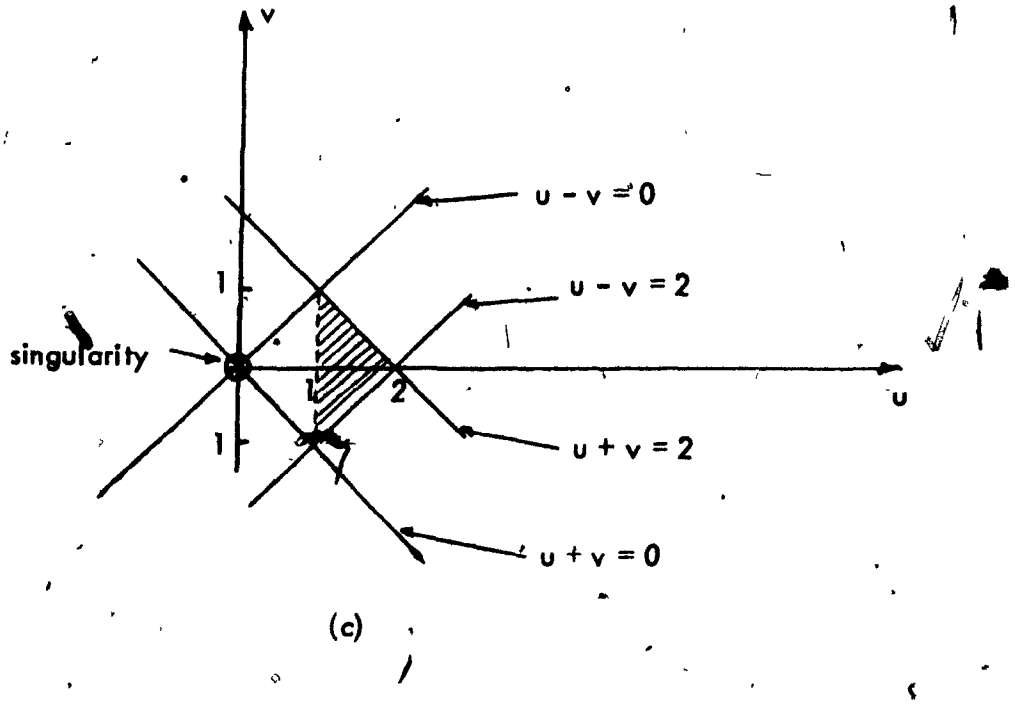

FIGURE 4.6 Transformation from $(s_m - s_n)$ Plane to $(u - v)$ Plane used for the Two Collinear Wire Problem of (a).

together with the element of area

$$du\,dv = \frac{2}{S_m^2}\,ds_m\,ds_n$$

Equation (4.39) becomes

$$R_{mn}^2 = S_m^2\,(u^2 + (a_n/S_m)^2) \tag{4.41}$$

and the double integrals of (4,7) in region 1, P_{mn1}, of Figure 4.6(b) is

$$P_{mn1} = \int_{u=0}^{u=1} \int_{v=-u}^{v=u} \frac{1}{2\,S_m^3} \cdot \frac{1}{\left(u^2 + \left(\frac{a_n}{S_m}\right)^2\right)^{2.5/2}}\, g(u,v)\,dv\,du$$

$$+ \int_{u=1}^{u=2} \int_{v=u-2}^{v=-u+2} \frac{S_m^2}{2}\, K(u,v)\,dv\,du \,, \tag{4.42}$$

where $K(u,v)$ and $g(u,v)$ are given by (4.13) and (4.26) respectively.

The integrand of the second term of (4.42) is smooth and continuous everywhere, so a Gauss-Legendre formula is used to carry out the integration with respect to u. The integration with respect to v is evaluated using a Gauss-Legendre formula at each quadrature node in the u direction.

The region of integration of the first term in (4.42) contains the singularity. Gauss-Christoffel is used in the u direction, and Gauss-Legendre in the v direction is also evaluated at each quadrature node in the u direction.

When two collinear wires are carrying currents in the same direction, Figure 4.7(a), Region (2) of Figure 4.7(b), is handled as before, while Region (1) is treated as follows.

In this case,

$$R_{mn}^2 = (s_n - s_m)^2 + a_n^2 \tag{4.43}$$

Using the following transformation,

$$\begin{aligned} u &= (s_n - s_m)/S_m \\ v &= (s_n + s_m)/S_m \end{aligned} \tag{4.44}$$

and the element of area (4.40), Equation (4.43) reduces to the expression (4.41), and P_{mn1} can be easily derived.

$$P_{mn1} = \int_{u=0}^{u=1} \int_{v=-u+2}^{v=u+2} \frac{1}{2 S_m^3} \cdot \frac{1}{\left(u^2 + \frac{a_n^2}{S_m^2}\right)^{5/2}} g(u,v)\, dv\, du$$

$$+ \int_{u=1}^{u=2} \int_{v=u}^{v=-u+4} \frac{S_m^2}{2} K(u,v)\, dv\, du \tag{4.45}$$

Evaulation of the integrals appearing in (4.45) is exactly the same as explained above.

Another case of interest, when the currents are directed towards the junction, as shown in Figure 4.8(a), is considered here. In the present case, Region (2) is treated as before. In Region (1) we have to use the transformation (4.40). Thus, P_{mn1} has the value,

$$P_{mn1} = \int_{u=b_2}^{b_3} \int_{v=u-2}^{v=\frac{2}{S_m}(S_n-u)} \frac{1}{2S_m^3} \cdot \frac{1}{(u^2+(\frac{a_n}{S_m})^2)^{5/2}} \cdot g(u,v)\, dv\, du + \int_{u=b_1}^{b_2} \int_{v=-u+\frac{2}{S_m}(S_n-S_m)}^{v=u} \cdot \frac{S_m^2}{2} K(u,v)\, dv\, du \qquad (4.46)$$

where the constants b_1, b_2 and b_3 have the values

$$b_1 = \frac{1}{S_m}(S_n - S_m)$$

$$b_2 = \frac{1}{S_m} S_n$$

$$b_3 = \frac{1}{S_m}(S_n + S_m)$$

These integrals are efficiently evaluated as Equations (4.42) and (4.45).

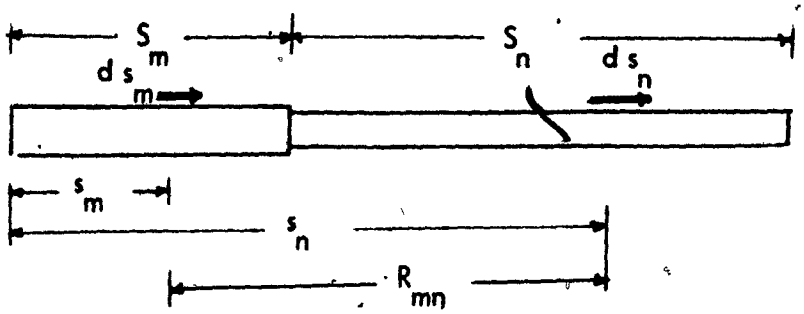

(a)

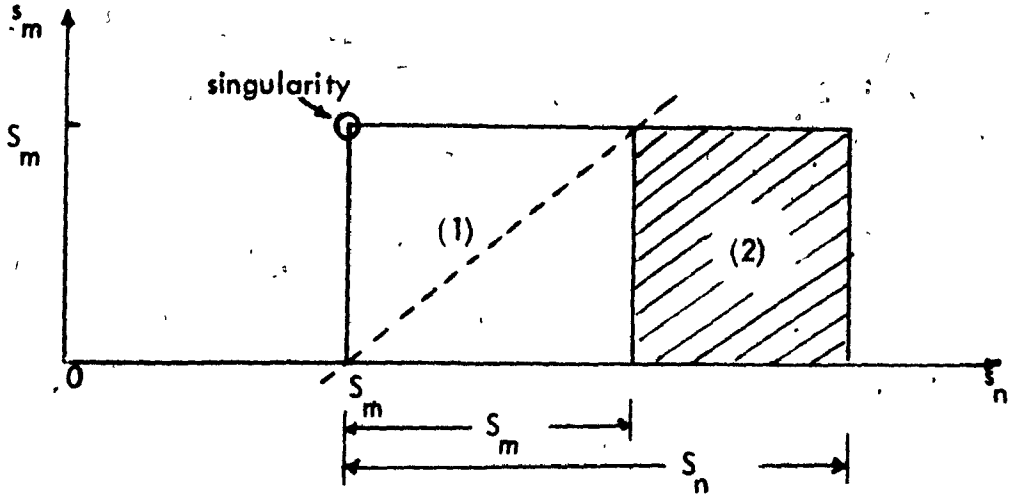

(b)

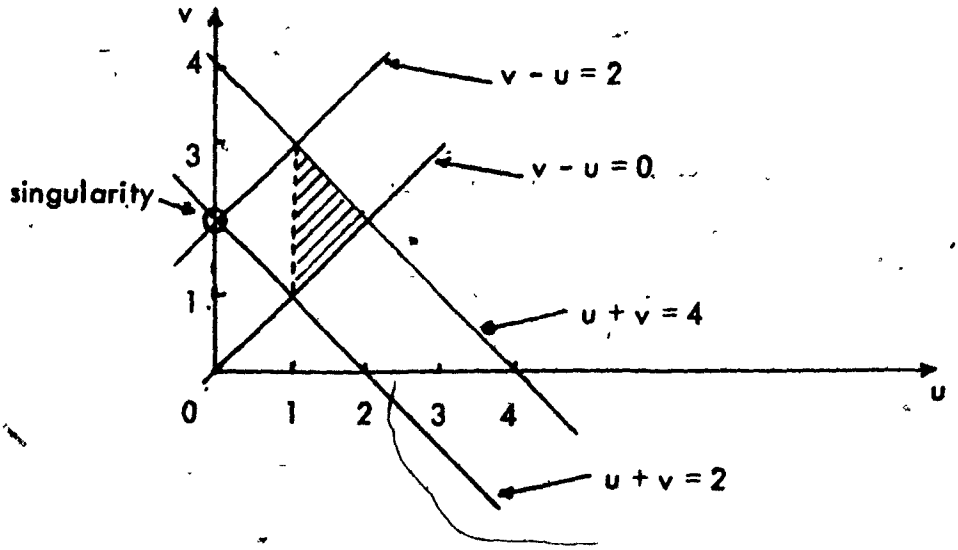

(c)

FIGURE 4.7 Transformation from $(s_m - s_n)$ Plane to $(u - v)$ Plane used for the Two Collinear Wire Problem of (a).

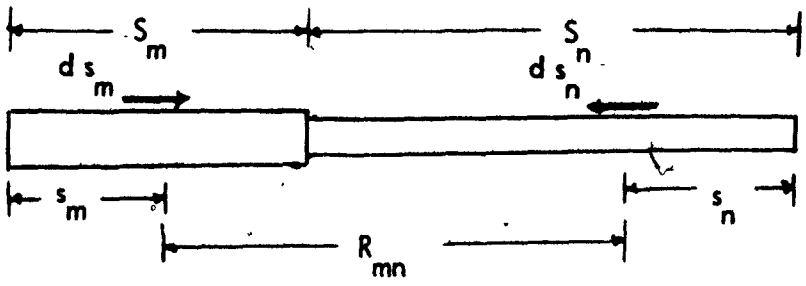

(a)

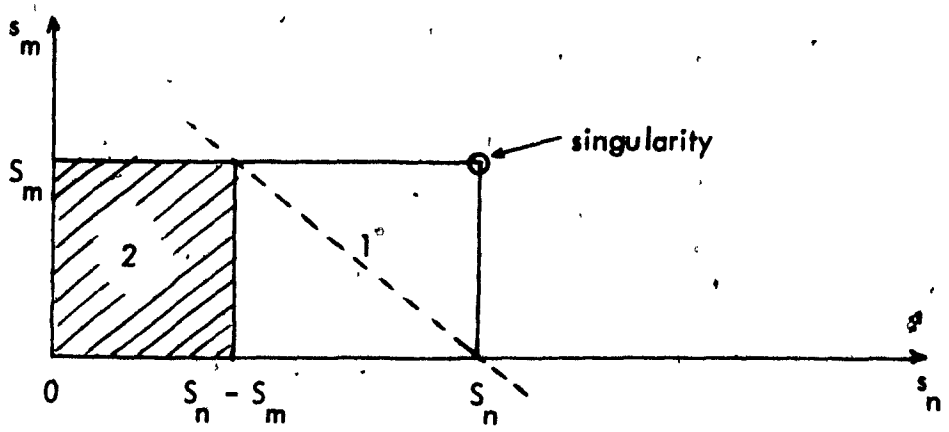

(b)

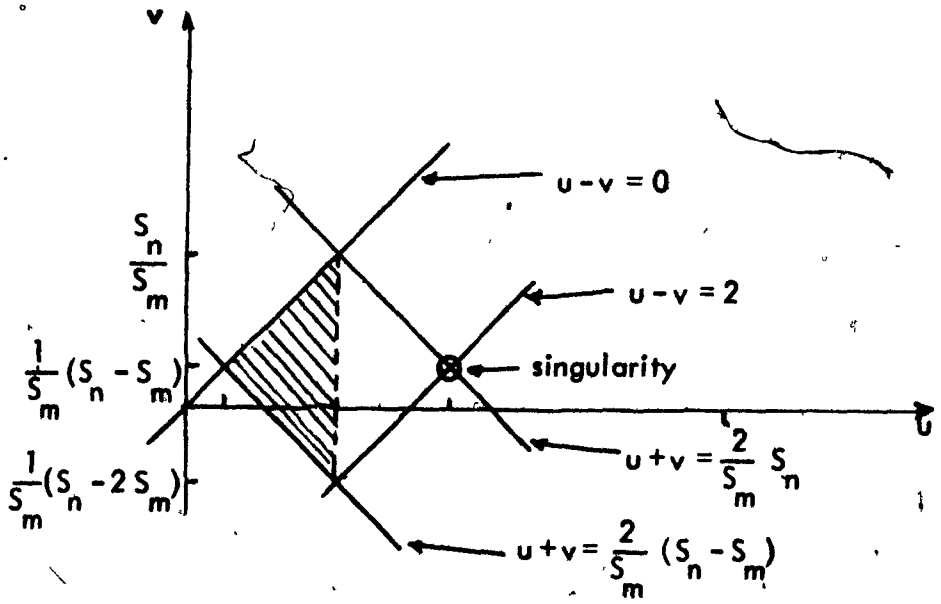

(c)

FIGURE 4.8 Transformation from $(s_m - s_n)$ Plane to $(u - v)$ Plane, used for the Two Collinear Wire Problem of (a).

4.3 Determination of the Excitation Matrix

The solution of (4.8) requires a knowledge of the complex current coefficients. These can be determined by solving Equation (3.43). In this equation, the right hand side

$$\text{R.H.S.} = \int_0^{S_n} \hat{n} \cdot \bar{E}^{im}(s_n)\, f_i(s_n)\, d s_n \qquad \begin{matrix} i=1, \ldots, L(n) \\ n=1, \ldots, N \end{matrix} \tag{4.47}$$

where L is the number of interpolation nodes of the n^{th} wire,

N is the number of wires,

is general in the sense that both radiation and scattering may be considered. Here, the solution of the scattering problem is obtained by taking the impressed field E^{im} of (4.47) as the incident electric field. (4.47) should be evaluated for N wires at $L(1) + L(2) + \ldots L(N)$ nodes.

Consider, the wire shown in Figure 4.9(a). The wire end coordinates are (x_1, y_1, z_1) and (x_2, y_2, z_2) and the current flow is indicated by the arrow. Also, let us take a linearly polarized plane wave travelling in some arbitrary direction $\hat{n}$ with respect to the cartisian axes. This is illustrated in Figure 4.10. The impressed field E^{im} at a point s_n on wire n, is given by

$$E^{im}(s_n) = (\hat{u}_1 E_1 + \hat{u}_2 E_2) \exp(-j k \hat{u} \cdot r) \tag{4.48}$$

where

$k = \frac{2\pi}{\lambda}$, the wave number

$$r = x_n \hat{a}_x + y_n \hat{a}_y + z_n \hat{a}_z$$

x_n, y_n, z_n are the cartesian coordinates of s_n

E_1 and E_2 are the electric field components in $\hat{u}_1$ and $\hat{u}_2$ directions respectively. They are normal to each other and lie on the plane of the wave.

$\hat{u}$ is the unit vector normal to the plane of the wave and can be expressed, in terms of the unit vectors $\hat{a}_x$, $\hat{a}_y$, $\hat{a}_z$ as

$$\hat{u} = \cos A \hat{a}_x + \cos B \hat{a}_y + \cos C \hat{a}_z$$

A, B and C are the angles that the unit vector $\hat{n}$ makes with the positive x, y and z axes respectively.

The dot product of r and u has the value

$$\hat{u} \cdot r = x_n \cos A + y_n \cos B + z_n \cos C \qquad (4.49)$$

If E_1 is equal to zero, the wave is linearly polarized in $\hat{u}_2$ direction.

If E_2 is equal to zero, the wave will be polarized in $\hat{u}_1$ direction. However, if E_1 and E_2 are both real or complex with equal phase, we have linear polarization in the direction $(\tan^{-1} \frac{E_2}{E_1}$ with $\hat{u}_1)$ of the resultant $(\sqrt{E_1^2 + E_2^2})$.

If E_1 and E_2 are both complex vectors having the components E_{1x}, E_{1y}, E_{1z} and E_{2x}, E_{2y}, E_{2z} in the x, y and z axes respectively, they can be represented by

$$\bar{E}_1 = E_{1x}\hat{a}_x + E_{1y}\hat{a}_y + E_{1z}\hat{a}_z$$

$$\bar{E}_2 = E_{2x}\hat{a}_x + E_{2y}\hat{a}_y + E_{1z}\hat{a}_z \qquad (4.50)$$

With this choice, we can make our scattering analysis more general and hence it can be used for linear, planar and three-dimensional wire structure.

Substitution of (4.48)-(4.50) into (4.47) we get

$$\text{R.H.S.} = C \int_0^{S_n} \exp\left[-jk(x_n \cos A + y_n \cos B + z_n \cos C)\right] f_i(s_n)\, d s_n \qquad (4.51)$$

where the constant C is given by

$$C = \left(\frac{x_1 - x_2}{S_n}\right)(E_{1x} - E_{2x}) + \left(\frac{y_1 - y_2}{S_n}\right)(E_{1y} - E_{2y}) + \left(\frac{z_1 - z_2}{S_n}\right)(E_{1z} - E_{2z})$$

and x_n, y_n and z_n can be expressed in terms of s_n as

$$x_n = \frac{x_1 - x_2}{S_n} s_n$$

$$y_n = \frac{y_1 - y_2}{S_n} s_n$$

$$z_n = \frac{z_1 - z_2}{S_n} s_n$$

This is illustrated in Figure 4.9(b). Making use of the following transformation

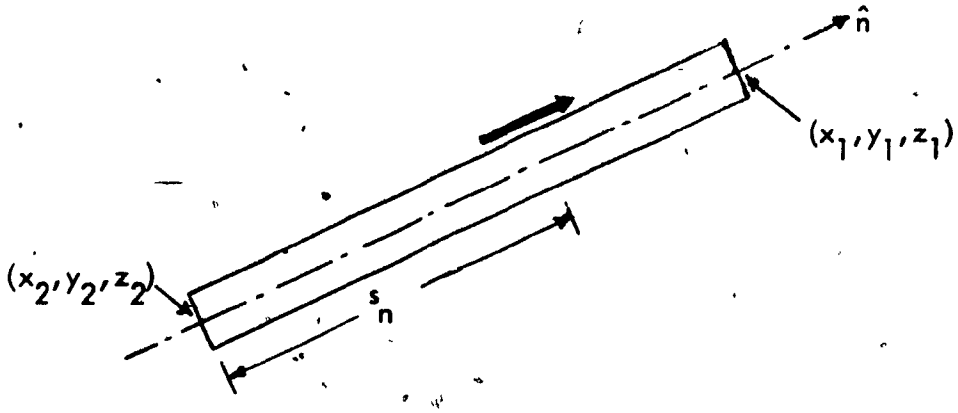

(a)

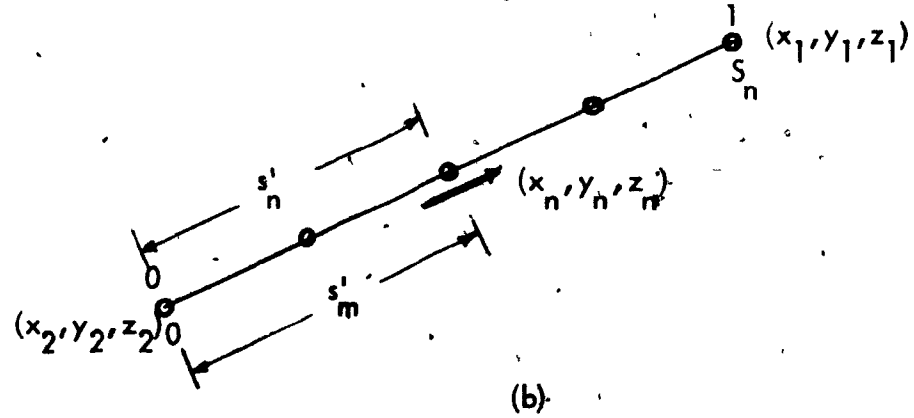

(b)

FIGURE 4.9 (a) A Single Wire.
(b) Interpolation Nodes.

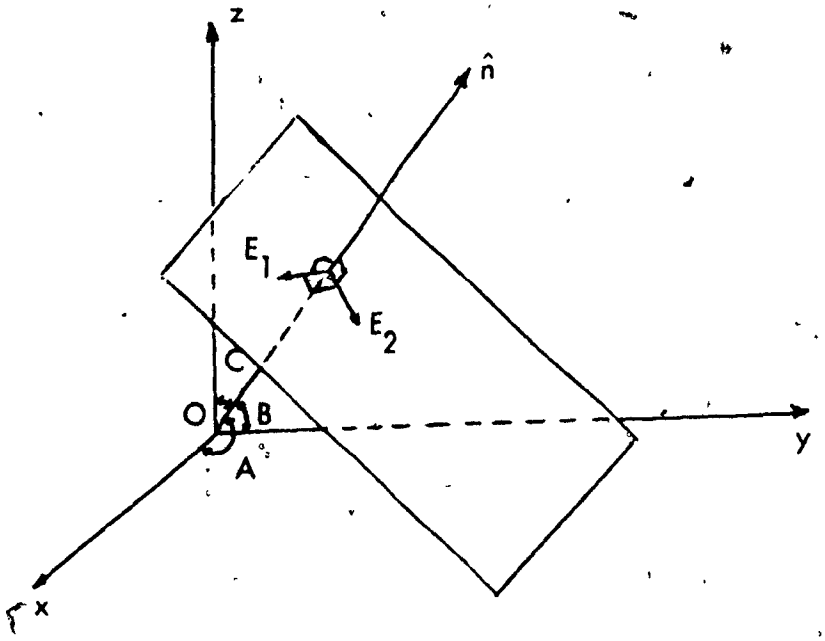

FIGURE 4.10 A Plane Wave Traveling in an Arbitrary Direction $\hat{n}$.

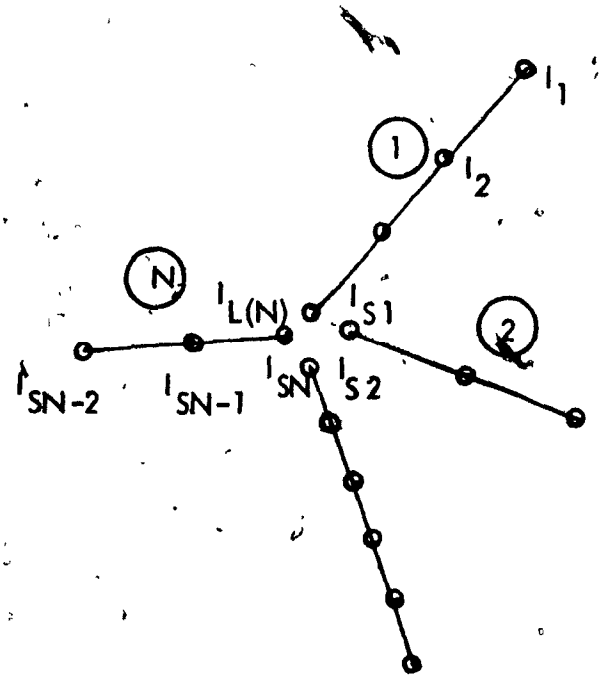

FIGURE 4.11 A Wire Junction.

$$s' = s/S_n \quad \text{and} \quad ds' = \frac{1}{S_n} ds \tag{4.52}$$

Equation (4.51) becomes

$$\text{R.H.S.} = S_n C \int_0^1 \exp(-jkT)\, f_1(S_n s_n)\, ds_n \tag{4.53}$$

where

$$T = (x_1 - x_2) s_n \cos A + (y_1 - y_2) s_n \cos B + (z_1 - z_2) s_n \cos C$$

The integrand of (4.53) is smooth, thus the integration is efficiently evaluated by Gauss-Legendre quadrature formula.

Now, substitution of the results of both sections 4.2 and 4.3 into (3.44), (3.44) can be easily solved for the unknown current coefficients. However, reduction of the number of unknown coefficients can be obtained as explained next.

4.4 Current Distribution on Interconnected Wires

Although, a complete analysis to deal with scattering by arbitrary configuration of wires has been given, yet the present thesis aims at the solution of interconnected wires of arbitrary orientations. At any junction, we have to satisfy Kirchhoff's current law. This can be achieved by following the treatment used by Silvester and Chan [19].

Consider a junction of N wires as shown in Figure 4.11. Let L(n) be the number of interpolation nodes on the n^{th} wire, the total number of nodes is

$$SN = \sum_{n=1}^{N} L(n)$$

To satisfy Kirchhoff's current law at the junction of Figure 4.11, we have

$$I_{S1} + I_{S2} + \ldots + I_{SN} = 0 \qquad (4.54)$$

where I_{SI} is the current coefficient of the last node of the i^{th} wire and

$$SI = \sum_{n=i}^{N} L(n)$$

Equation (4.54) reduces the number of unknowns by one.

The relation between the interpolation coefficients of the conjoint structure and that of the corresponding disjoint structure can be obtained if we consider (4.54) as a mapping of the SN - 1 unknowns of the conjoint structure into the SN unknowns of the disjoint structure.

$$\begin{bmatrix} I_1 \\ I_2 \\ \vdots \\ I_{SN-1} \\ I_{SN} \end{bmatrix} = \begin{bmatrix} 1 & 0 & 0 & \cdots & 0 \\ 0 & 1 & 0 & \cdots & 0 \\ & & & & \\ 0 & 0 & 0 & \cdots & 1 \\ 0 & 0 & -1 & \cdots & -1 \end{bmatrix} \begin{bmatrix} I_1 \\ I_2 \\ \vdots \\ I_{SN-1} \end{bmatrix} \qquad (4.55)$$

where the first (-1), in the last row is located in the 51^{th} column and the last (-1) is located in the SN^{th} column.

The matrix equation of (4.55) is

$$I^{dis} = C\, I^{con} \tag{4.56}$$

Substitution of (4.56) into (3.44) of the disjoint structure, and premultiplication by C^T, we get

$$(C^T Z^{dis} C)\, I^{con} = C^T V^{dis} \tag{4.57}$$

or

$$Z^{con}\, I^{con} = V^{con} \tag{4.58}$$

where

$$Z^{con} = C^T Z^{dis} C \tag{4.59}$$

$$V^{con} = C^T V^{dis} \tag{4.60}$$

Equation (4.58) is solved to get the unknown current coefficients $I_1, I_2, \ldots I_{SN-1}$. Thus the current distributions can be obtained.

4.5 Far Field and Radar Cross-section Patterns of Interconnected Wires

Once the current distributions on the wires are known, the far field pattern and hence the radar cross-section pattern are easily determined. Here,

the approach derived by Chan [5] is briefly discussed.

An arbitrarily located wire of length $2h_m$ is considered. The coordinates of the centre is (x_m, y_m, z_m). Its unit vector is,

$$\hat{m} = \hat{x} \cos\alpha_m \cos\beta_m + \hat{y} \cos\alpha_m \sin\beta_m + \hat{z} \sin\alpha_m$$

where

α_m is the angle between the wire and its projection on the x-y plane

β_m is the angle between this projection and the x-axis

Assume a very far field point (r, θ, ϕ), so that only the radiation field is obtained.

$$E_\theta = -jw\mu \overline{A}_m \hat{\theta}$$

$$E_\phi = -jw\mu \overline{A}_m \hat{\phi} \qquad (4.61)$$

$$E_r = 0$$

Let the current be approximated by $I^m(s_m) = \sum_{i=1}^{L} I_i^m f_i^m(s_m)$ where L is the number of interpolation nodes on element m.

Evaluation of the magnetic vector potential $\overline{A}_m$ at the field point due to element m, and substituting the resulting expression into (4.61), we get

$$E_\theta(r,\theta,\phi) = -j\omega\mu \frac{\exp(-jkr)}{4\pi r} h_m \exp(j\upsilon) \sum_{i=1}^{L} I_i^m \int_{-1}^{1} f_i(s_m^i)$$

$$e^{jvs_m} \, ds_m \cdot [\cos\beta_m \cos\alpha_m \cos\theta \cos\phi + \sin\beta_m \cos\alpha_m \sin\phi \cos\theta - \sin\alpha_m \sin\theta] \qquad (4.62)$$

$$E_\phi(r,\theta,\phi) = -j\omega\mu \frac{\exp(-jkr)}{4\pi r} h_m \exp(j\upsilon) \sum_{i=1}^{L} I_i^m \int_{-1}^{1} f_i(s_m^i)$$

$$e^{jvs_m} \, ds_m \cdot [-\cos\beta_m \cos\alpha_m \sin\phi + \sin\beta_m \cos\alpha_m \cos\phi] \qquad (4.63)$$

where

$$u = k(x_m \sin\theta\cos\phi + y_m \sin\theta\sin\phi + z_m \cos\theta)$$

$$v = k h_m(\sin\theta\cos\phi\cos\beta_m \cos\alpha_m + \sin\theta\sin\phi\cos\alpha_m \sin\beta_m + \cos\theta\sin\alpha_m)$$

The electric field due to N wires can be obtained from (4.62) and (4.63) by summing up all electric field components resulting from the individual wires, from 1 to N.

The radar cross-section of an obstacle is defined as the area for which the incident wave contains sufficient power to produce, by omnidirectional radiation, the same back-scattered power density. Its mathematical expression is

$$\sigma = \lim_{r\to\infty} \left(4\pi r^2 \frac{\bar{S}^s}{\bar{S}^i}\right) \qquad (4.64)$$

where

$$\bar{S}^s = \frac{1}{\eta} |E^s|^2, \text{ the scattered power density}$$

$$\bar{S}^i = \frac{1}{\eta} |E^i|^2, \text{ the incident power density} \tag{4.65}$$

Substitution of (4.62) and (4.65) into (4.64) results in

$$\sigma_{\theta\theta} = 4\pi \frac{|E_\theta^s|^2}{|E_\theta^i|^2} \tag{4.66}$$

or using (4.63), we get

$$\sigma_{\phi\theta} = 4\pi \frac{|E_\phi^s|^2}{|E_\theta^i|^2} \tag{4.67}$$

CHAPTER V

NUMERICAL INVESTIGATIONS

5.1 Introduction

In this chapter, the analytical investigation given in Chapter IV, is applied to solve several wire configurations. Computer programs have been written for analysing the electromagnetic behaviour of interconnected straight thin wires. Scattering problems only are solved. The current distribution is calculated by using Lagrangian interpolation polynomial approximation. Then, the far scattered field and the bistatic radar cross-section patterns, as well as the self and mutual impedances, are computed for some configurations. Almost all curves are drawn by using an H-P 7202A Graphic Plotter operating in parallel with a Tektronix 4010 terminal.

For the present plane wave scattering problem, a structure of arbitrarily located straight wires is illuminated by a known incident linearly polarized plane wave of arbitrary direction. The procedure presented here can be used to analyse linear, planar and three dimensional wire structures.

5.2 Numerical Results for Simple Problems

To illustrate the accuracy and the efficiency of the new method, several interconnected wire problems have been considered. In all these problems,

an incident plane wave of unity amplitude and polarized in the z-direction, is assumed to be propagating along the y-axis. The operating frequency is taken to be 150 megacycles. A second order polynomial approximates the currents on the wires.

First of all, the single wire whose axis coincides with the z-axis as shown in Figure 5.1, is analysed. The wire is half a wave length long with a radius a = .00350λ. The current distribution obtained, shown in Figure 5.2, is compared with the Kuo and Strait results [10]. The discrepancy between the two curves is due to the inaccurate results of Kuo and Strait. They performed numerically the integrations, appearing in the entries to the generalised inpedance matrix, by using a current approximation of the first order, i.e., piecewise linear approximation. Although a second order approximation suffices, the current is approximated here by Lagrangian interpolation polynomials of the third order to get an accurate current distribution.

We have mentioned in Chapter IV, that the present method is valid for very large angles between the interconnected wires, and for very small angles as well. This type of problem has never been analysed before. Very good results are obtained. These can be illustrated by the following examples.

The two collinear wires of Figure 5.3(a) are first considered. They are directed into the z-axis. The wire lengths and the radii are equal ($\ell = \lambda/4$, a = .0035λ). The currents are assigned the same reference direction. Two interconnected wires forming a very large angle, about 177.8 degrees, are considered next. The axis of the first wire coincides with the z-axis, while that

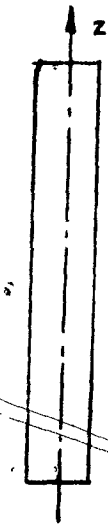

FIGURE 5.1 A Single Wire.

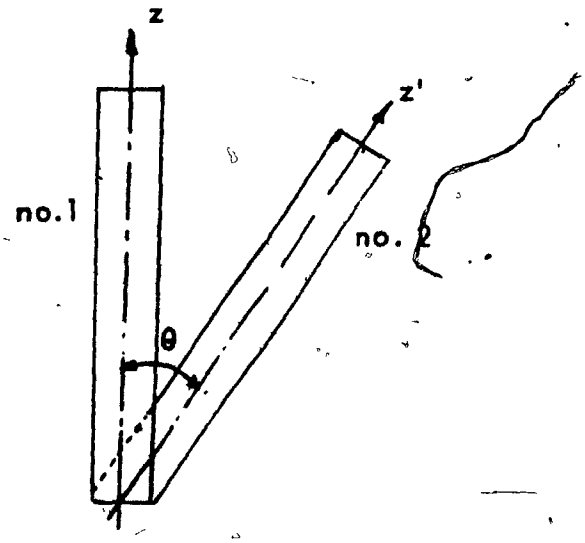

FIGURE 5.7 Two Connected Wires $\theta = 2.2^{\circ}$

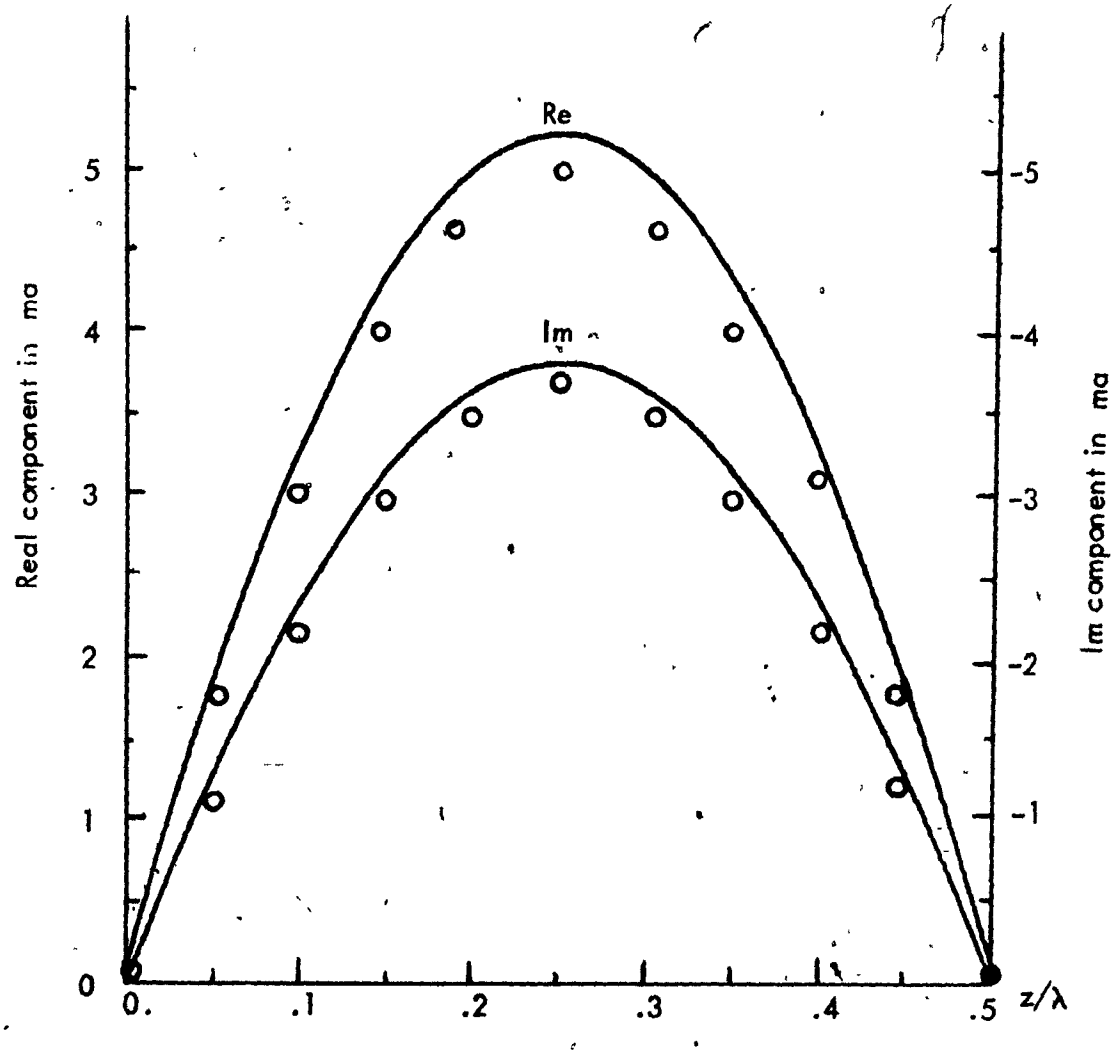

FIGURE 5.2 · Current Distribution on a Single Wire Scatterer $\ell = \lambda/2$, $a = .0035\,\lambda$.

—— This Method

O O Kuo and Strait

of the second wire is directed in the z'-axis, as shown in Figure 5.3(b). The same lengths and radii of the two collinear wire cases are taken. The same current reference directions are also assumed. Results of these two cases are compared in Figure 5.4, giving an agreement to the third decimal figure. Single precision is used throughout the whole program.

The two wires together having a total length of $\lambda/2$ give the same results as that obtained by the half wave length wire of Figure 5.1.

Again the same problem is repeated but with unequal lengths. Figures 5.3(c) and 5.3(d) show respectively, collinear wires and connected wires forming an angle of 177.8 degrees. In both cases, the first wire is 0.2λ in length, while the second is 0.3λ. Curves of the current distribution are illustrated in Figure 5.6. They agree with the results of the problems of Figures 5.1, 5.3(a), and 5.3(b).

The vertical far field pattern, for the case of two collinear wires, is illustrated in Figure 5.5. Since the current distribution is the same as for the single wire, the expected figure eight is obtained.

With these different methods and different analyses, which give the same results, one can expect the usefulness and the validity of the present method.

Figure 5.7 shows two interconnected wires forming a very small angle, about 2.2 degrees. They have equal lengths ($\ell=\lambda/2$) and radii ($a = .0035\lambda$) and are directed along the z and z'-axes. Current distribution is shown in Figure

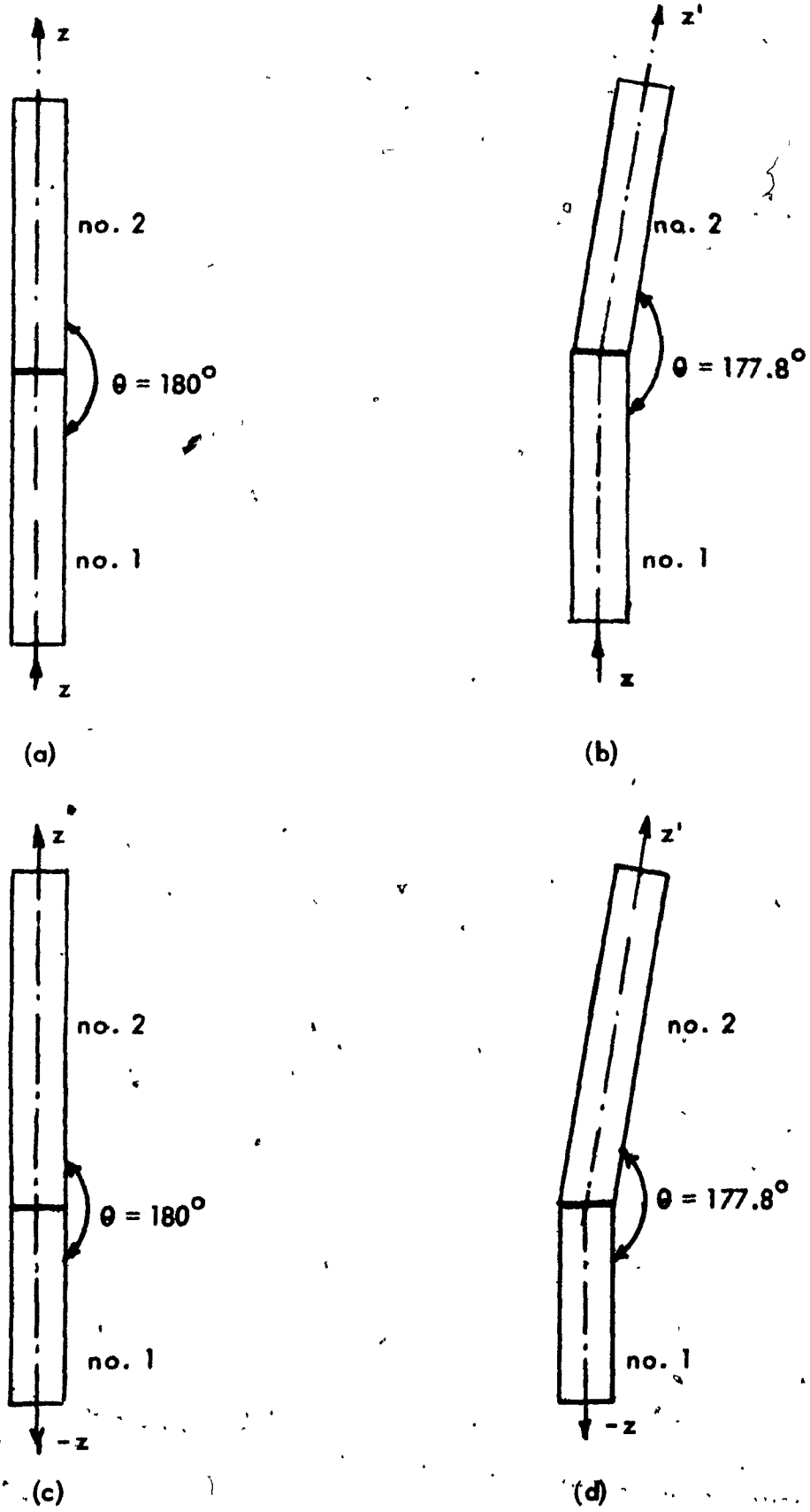

FIGURE 5.3 Collinear (a, c) and Connected (b, d) Wires with Equal and Unequal Lengths.

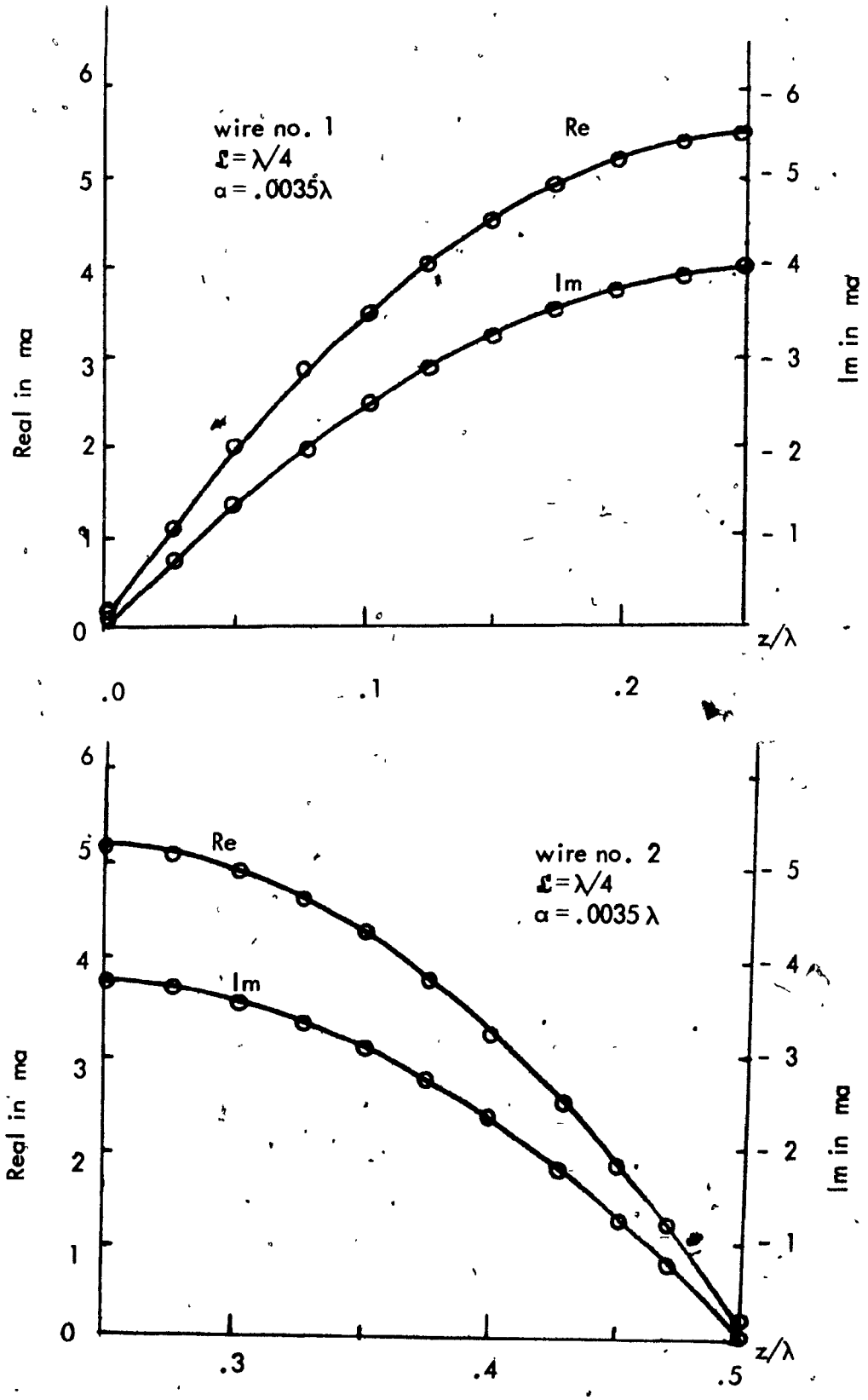

FIGURE 5.4 Current Distribution on Two Connected Wires of Equal Lengths.

—— Two Collinear Wires

OOO Two Connected Wires with $\theta = 177.8^0$

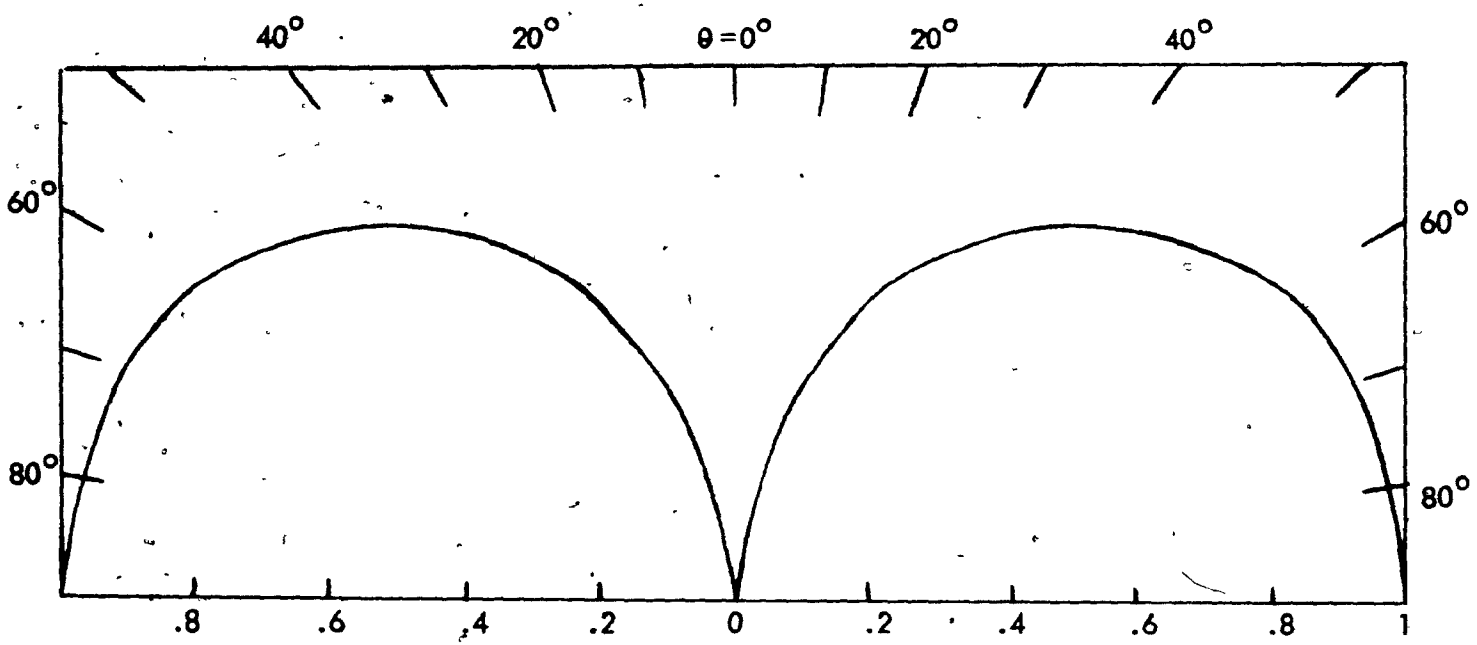

FIGURE 5.5 Vertical far Field Pattern for Two Collinear Wires of Equal Lengths.

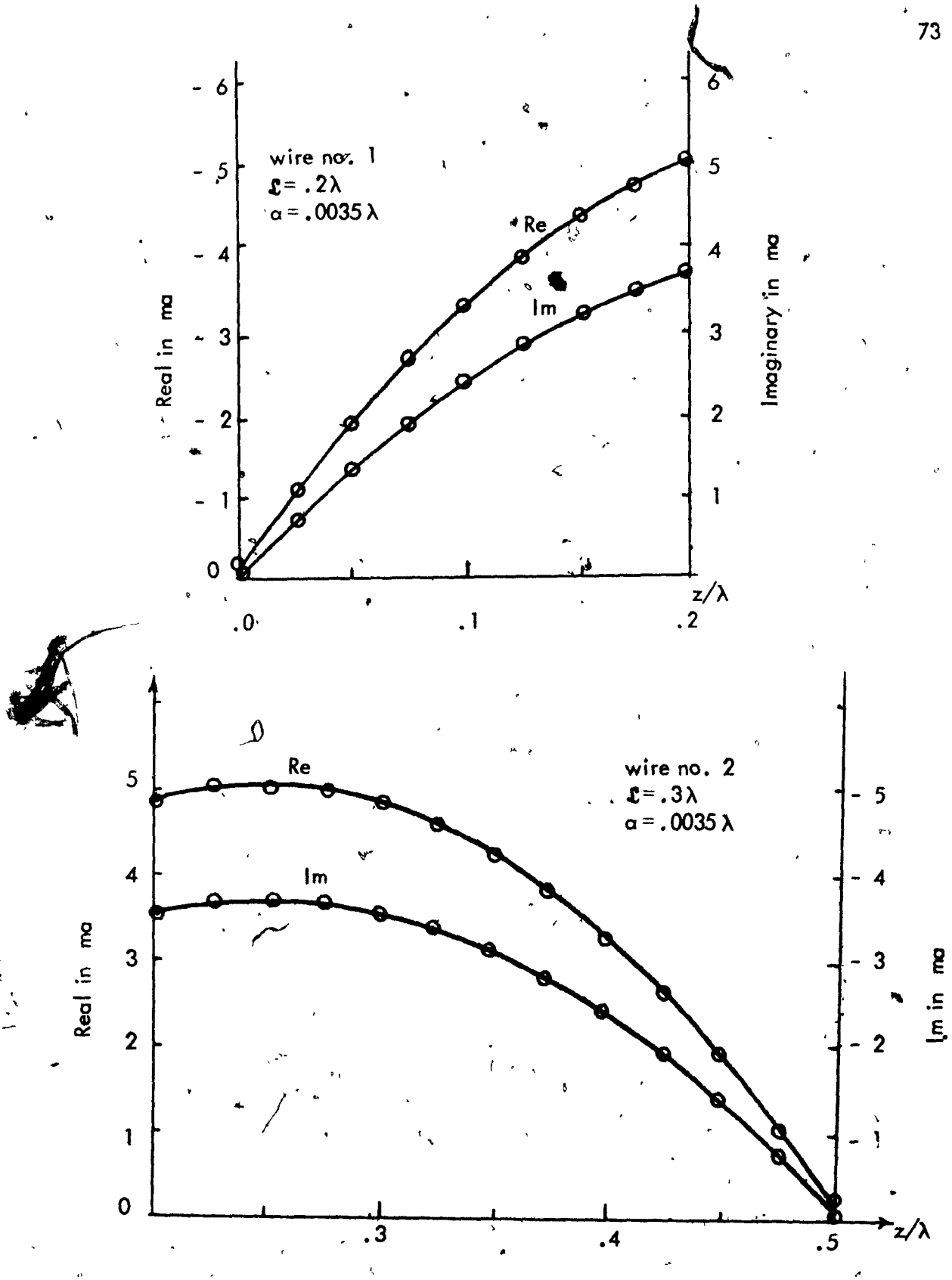

FIGURE 5.6 Current Distribution on Two Connected Wires of Unequal Lengths.

—— Two Collinear Wires

OOO Two Connected Wires with $\theta = 177.8^{\circ}$

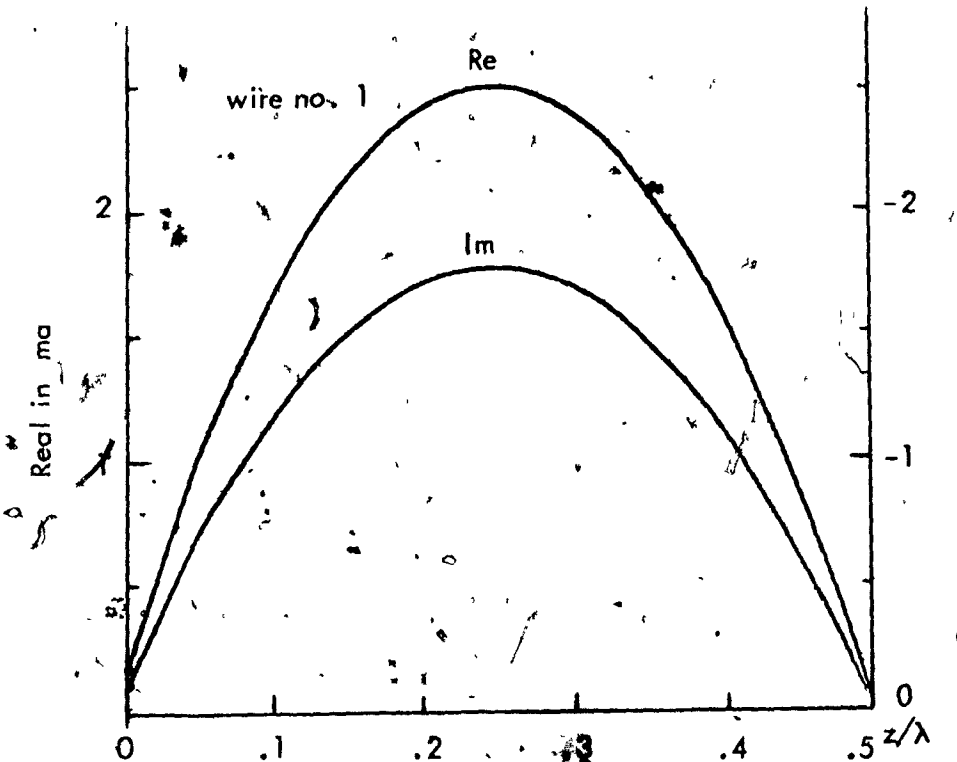

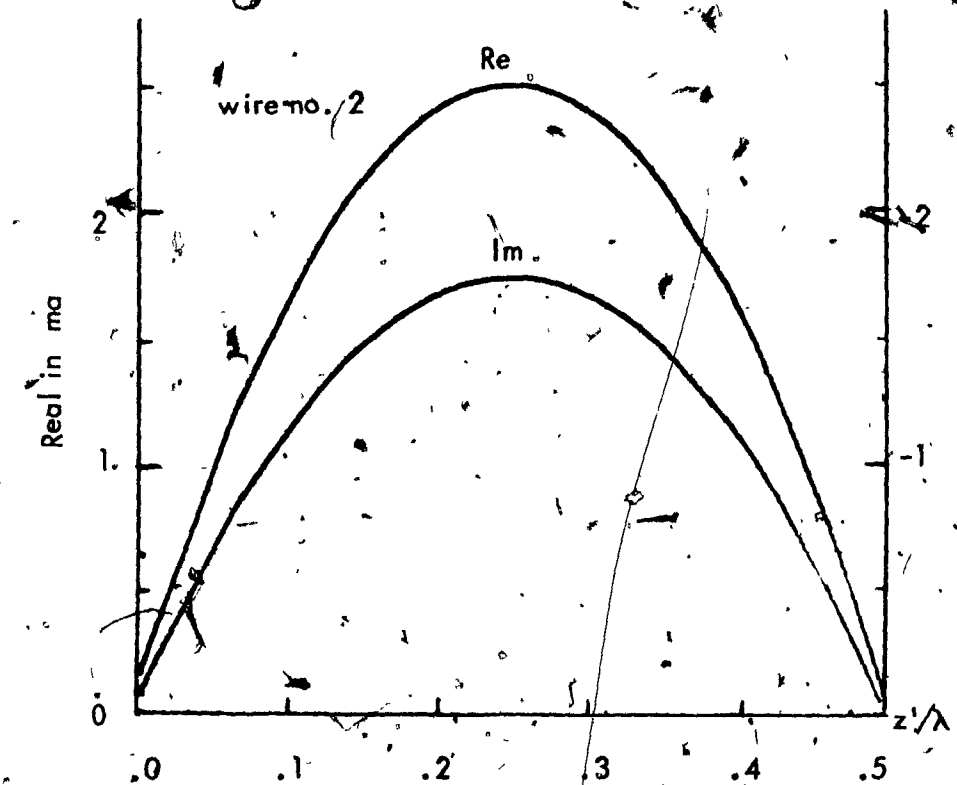

FIGURE 5.8 Current Distribution on Two Connected Wires of Equal Lengths. $\ell = \lambda/2$, $a = .0035\lambda$, $\theta = 2.2°$.

5.8. Here, the current obtained in each element is about half the current of a half wave length wire. This could be expected if we assume that this single wire is split into two wires connected at one end. Therefore, the current is distributed equally into the two wires giving half the single wire current.

Computation of the current distribution for such connected elements using second order polynomials takes about 3 seconds and for collinear wires about 0.75 seconds on the IBM 360/75.

5.3 Numerical Solution for Wire Structures

More complicated structures of interconnected wires are presented here., Results are compared with those of other investigators. Very good agreement is obtained. Some practical configurations of engineering interest are considered. In each case, an incident field of unity amplitude is taken. It is directed along the y-axis and polarized in the z-axis. The wavelength is one meter. A second order polynomial approximates the currents on all wires.

Scattering by the wire cross of Figure 5.9, has been analysed by Chan [5], Chao and Strait [2], Taylor et al [27] and Butler [1]. Its dimensions are $\ell_1 = \ell_2 = \ell_3 = 0.11\lambda$, $\ell_4 = 0.22\lambda$ and the radii are all the same and equal to 0.00222λ. The present method gives the same results as those of Butler and close results to those obtained by the other authors, as shown in Figure 5.10. Butler formulated Hallen's integral equation for the skew crossed wires. More accurate results are obtained by this method. Therefore we can conclude that the present

analysis is very accurate and is preferable to other methods. Also the bistatic radar cross-section, Figure 5.11, is computed in the plane $\varphi = 90^\circ$.

The special case of skew crossed wires when $\theta = 30^\circ$, of Figure 5.12, is also considered. The same dimensions, as for the case of $\theta = 90^\circ$ analysed above, are taken. Results are in good agreement with those of Butler. These are illustrated in Figure 5.13.

Figure 5.14 shows a T-scatterer of equal elements. The lengths are $\ell_1 = \ell_2 = \ell_3 = 0.11\lambda$ and radii $a_1 = a_2 = a_3 = 0.00222\lambda$. One can see from Figures 5.15 and 5.16 the current distribution obtained together with that of Kuo and Strait.

Finally, scattering by a three dimensional Brown wire structure is examined. Figure 5.17 illustrates this configuration illuminated by a plane wave polarized in the z-direction and of unity amplitude. It consists of four equal legs directed along the z, r, s, and t-axes. Each leg has a length ℓ wavelength, and a radius $\lambda/200$. The wavelength is taken to be one meter. The currents induced on the wires are plotted in Figure 5.18 for $\ell = 0.2$.

Nasu [30] analysed theoretically this Brown structure and got the input impedance against wire length. Numerical computation, using the present method, results in the curves shown in Figure 5.19 and compared with those of Nasu.

It is interesting to note that the current is not forced to be zero at the free end of the wire for any of the previous analyses. Acceptable zeros are obtained at these ends. Other methods consider a boundary condition by requiring the current to vanish at the free end of the wire.

The computation times needed for a T-scatterer and Brown structure are respectively 7 seconds and 15 seconds on the IBM 360/75. The execution time to find the input impedance for a Brown structure against a leg length is about 110 seconds. A completely different problem has to be solved every time the length is changed.

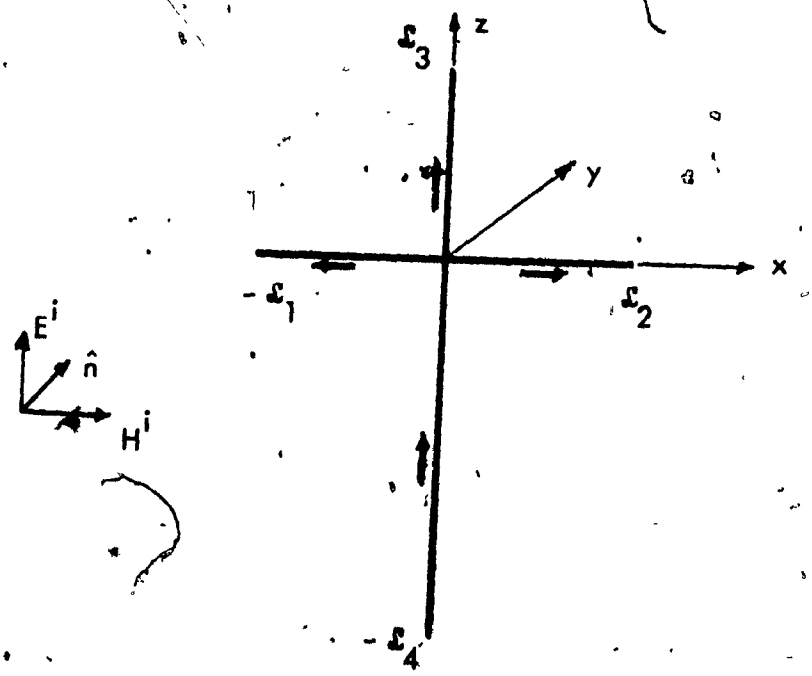

FIGURE 5.9 Wire Cross

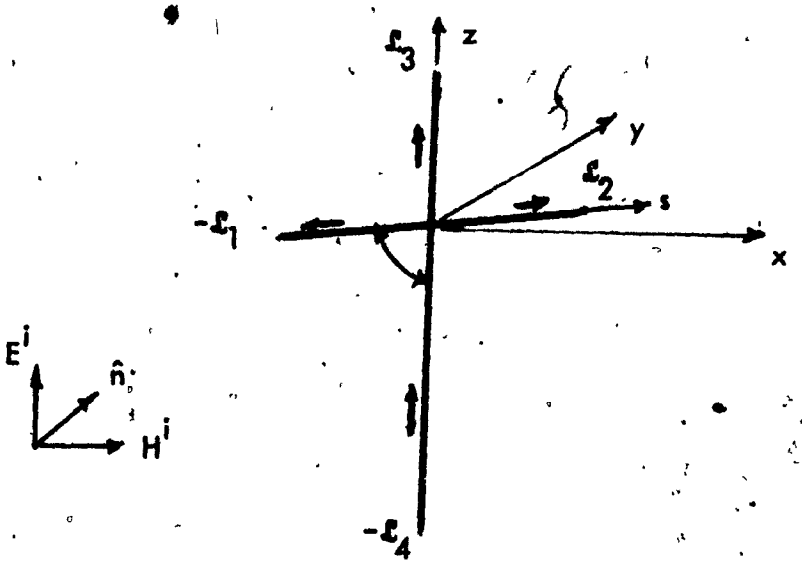

FIGURE 5.12 Skew Crossed Wires

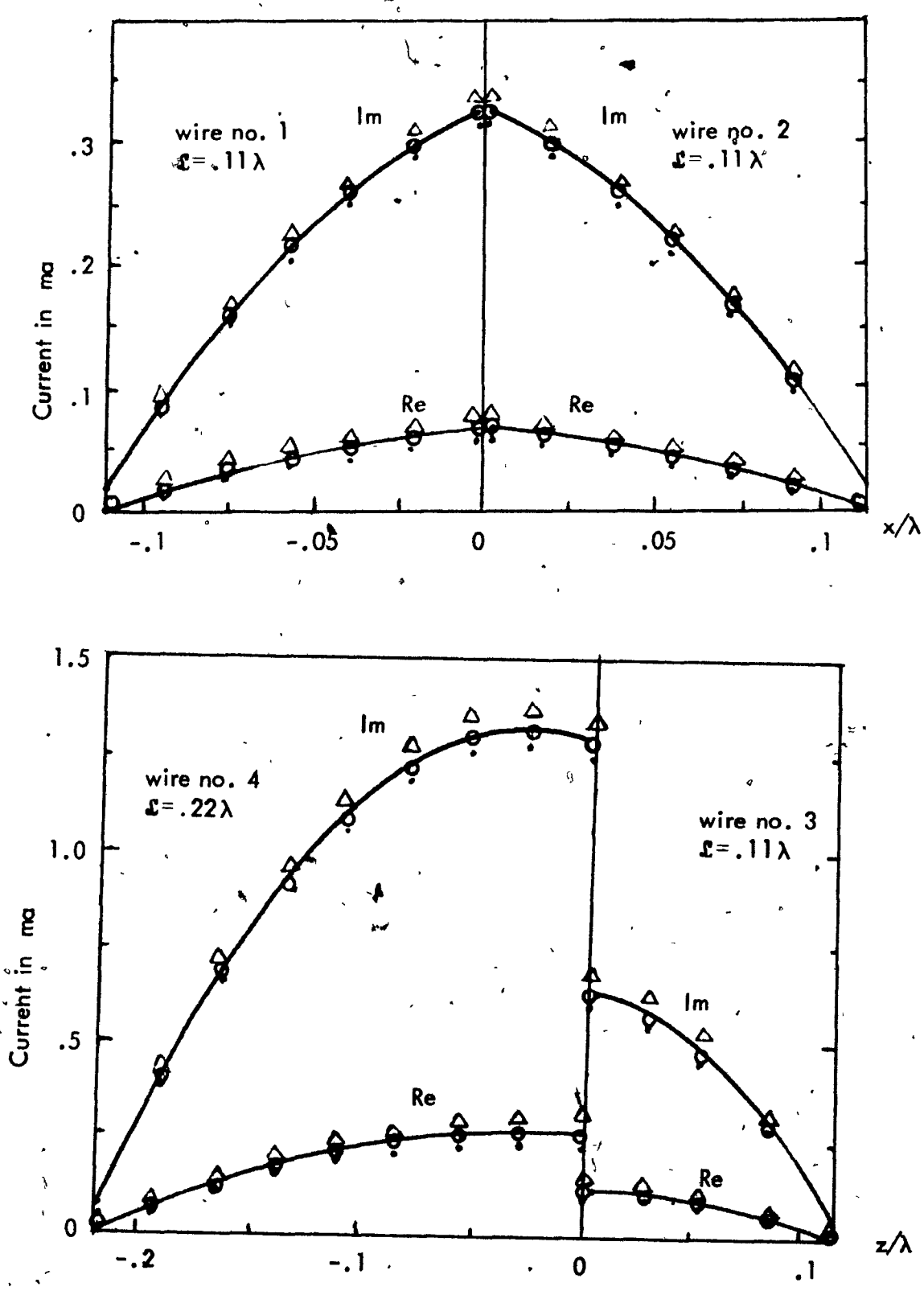

FIGURE 5.10 Currents on a Wire Cross ($a = .00222\lambda$).

—— This Method OOO Butler

. . . Chan, Chao and Strait ΔΔΔ Taylor

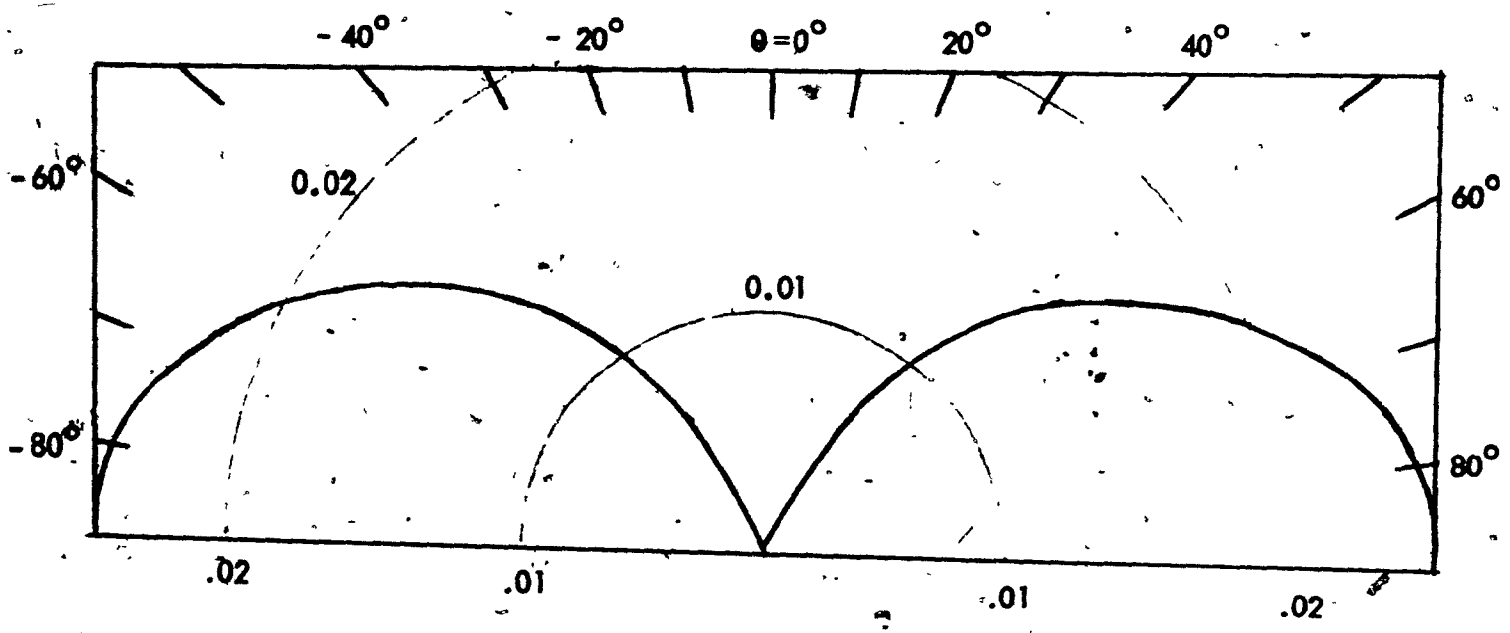

FIGURE 5.11 Bistatic Radar Cross-section $\sigma_{\theta\theta}/\lambda^2$ Pattern for the Wire Cross $\phi=90°$.

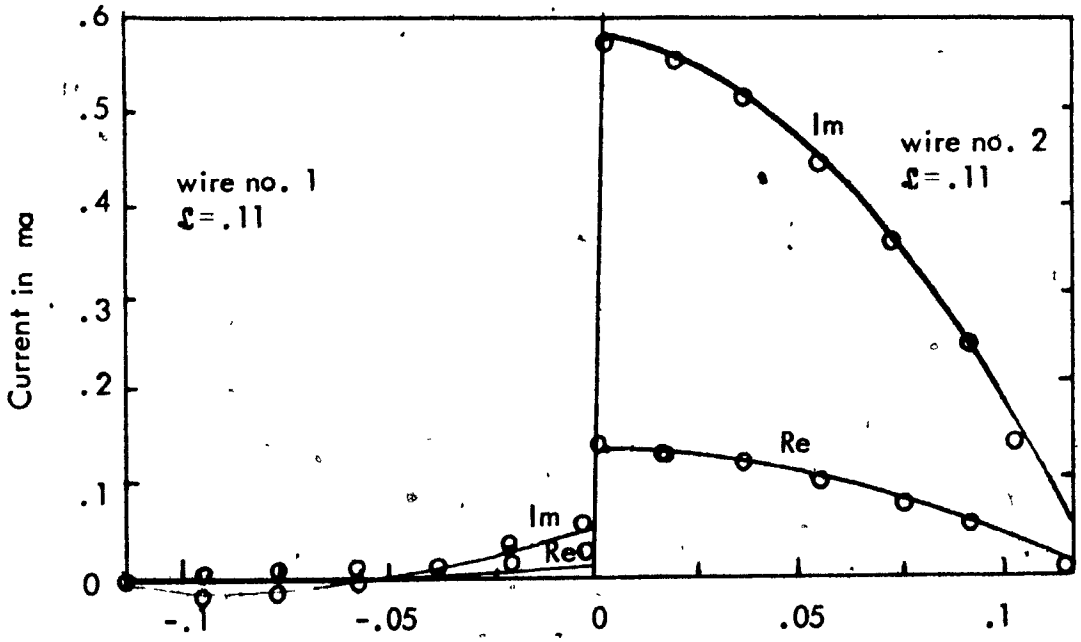

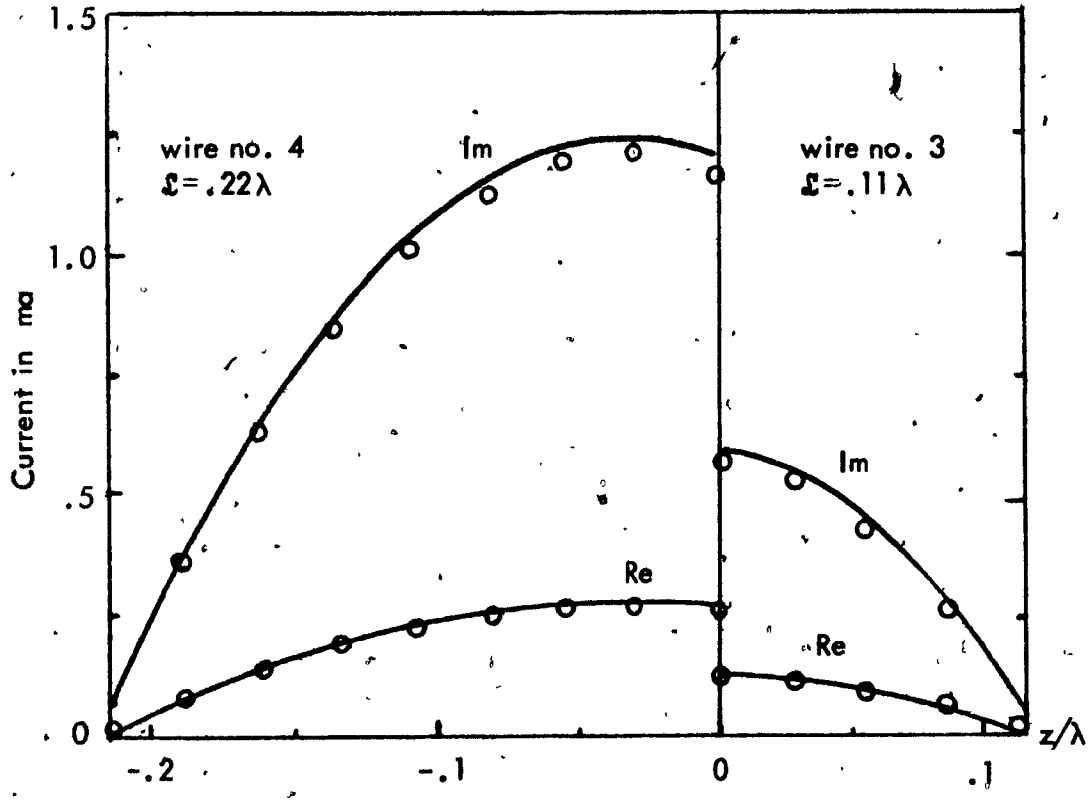

FIGURE 5.13 Currents on a Skew Crossed Wire (a = .00222λ).

—— This Method

OOO Butler

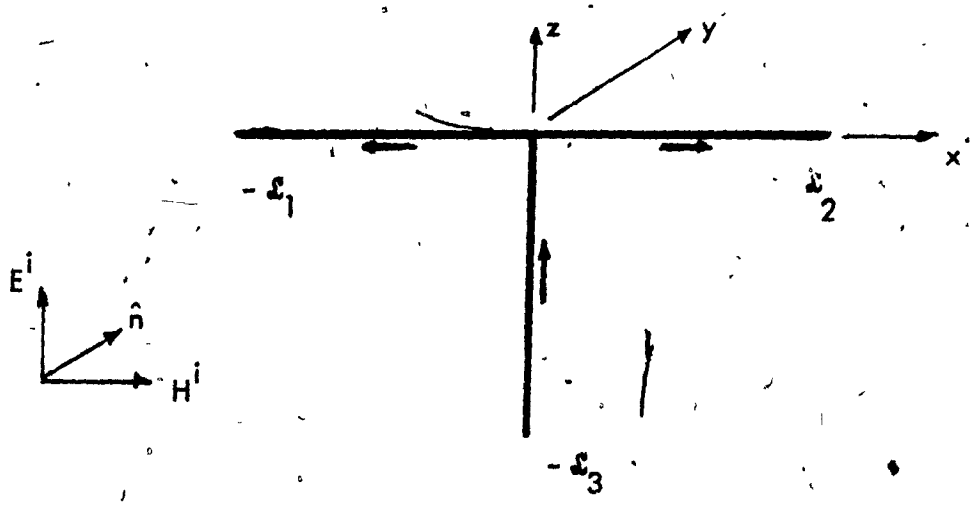

FIGURE 5.14 T-wire Scatterer.

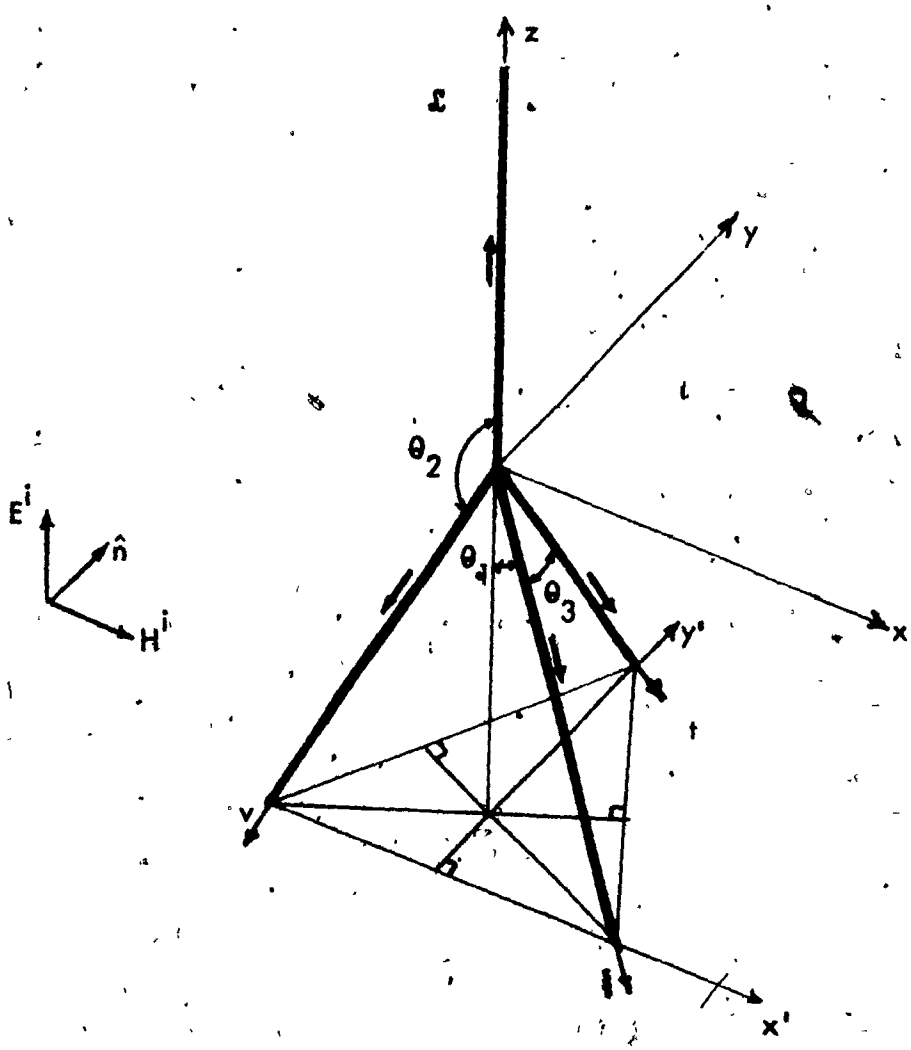

FIGURE 5.17 Three Dimensional Brown Wire Configuration.

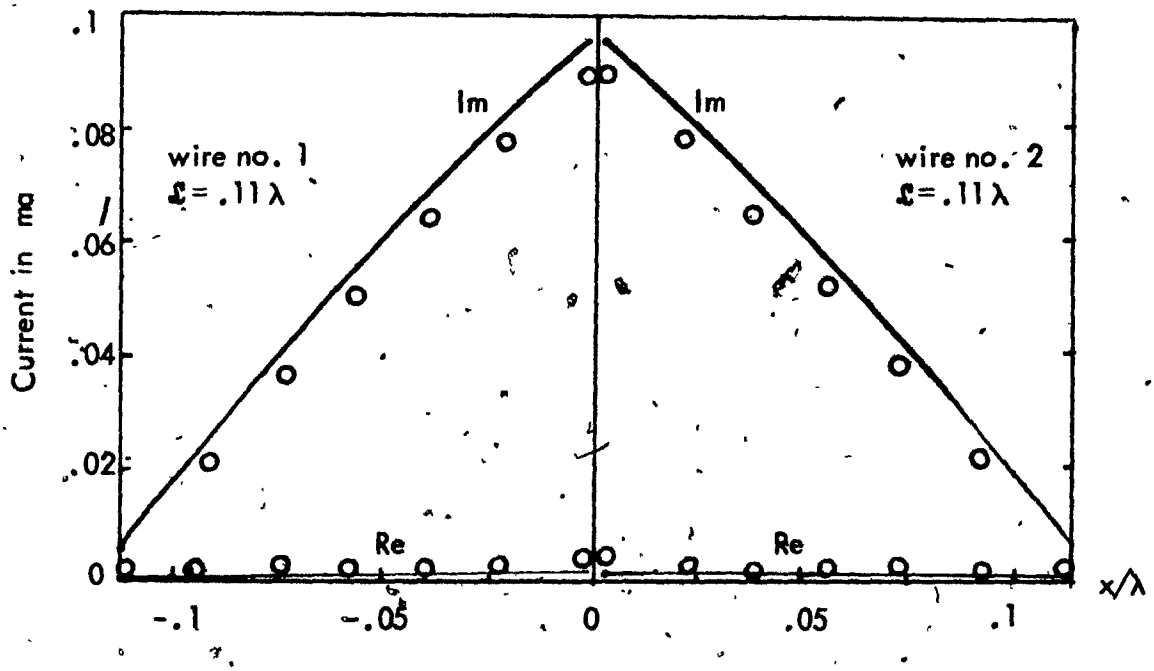

FIGURE 5.15 , Current Distribution on the Horizontal Curves of a T-scatterer, a = .00222λ

—— This Method

OOO Kuo and Strait

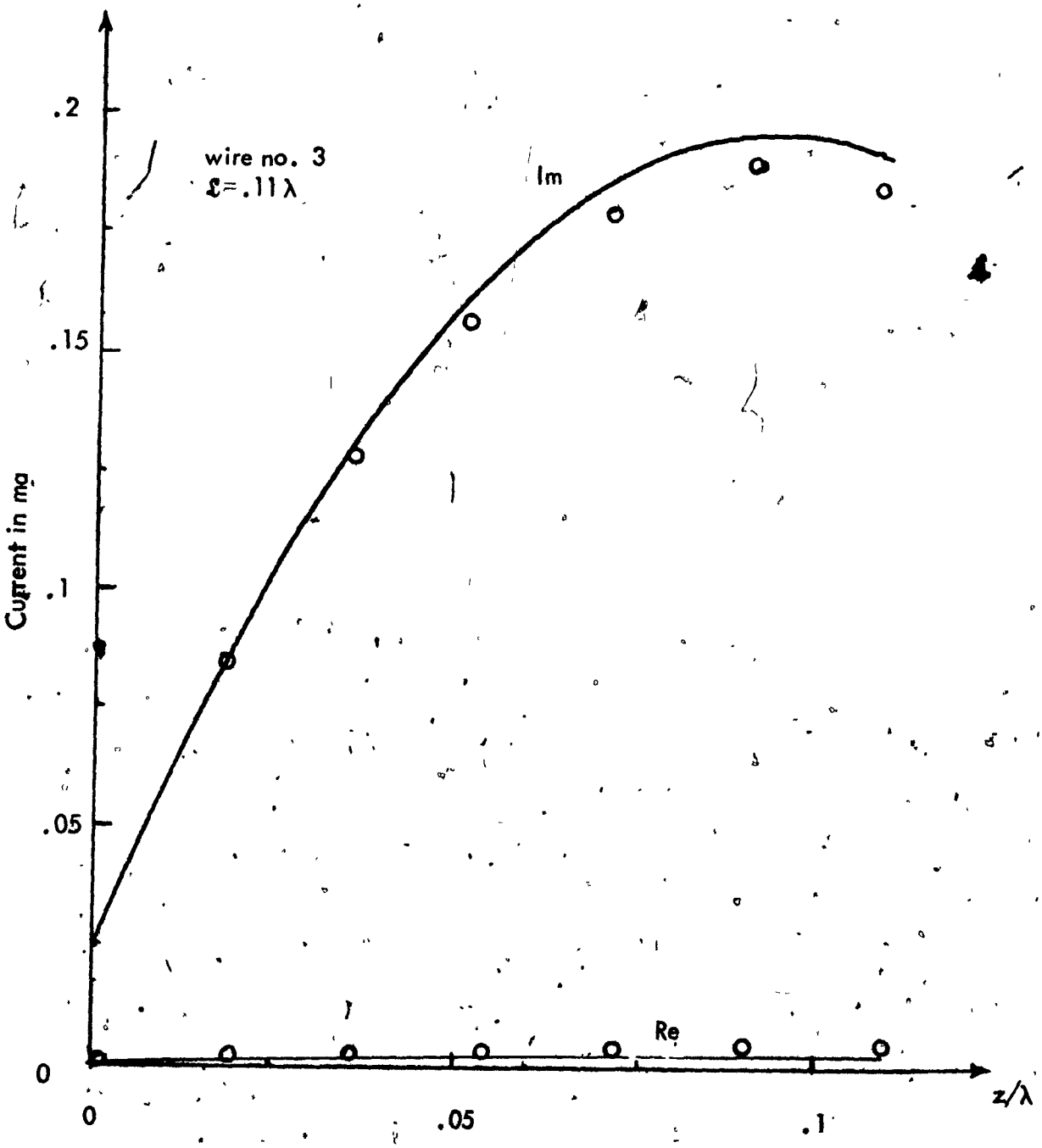

FIGURE 5.16 Current Distribution on the Vertical Wire of a T-scatterer, a = .00222 λ.

—— This Method

OOO Kuo and Strait

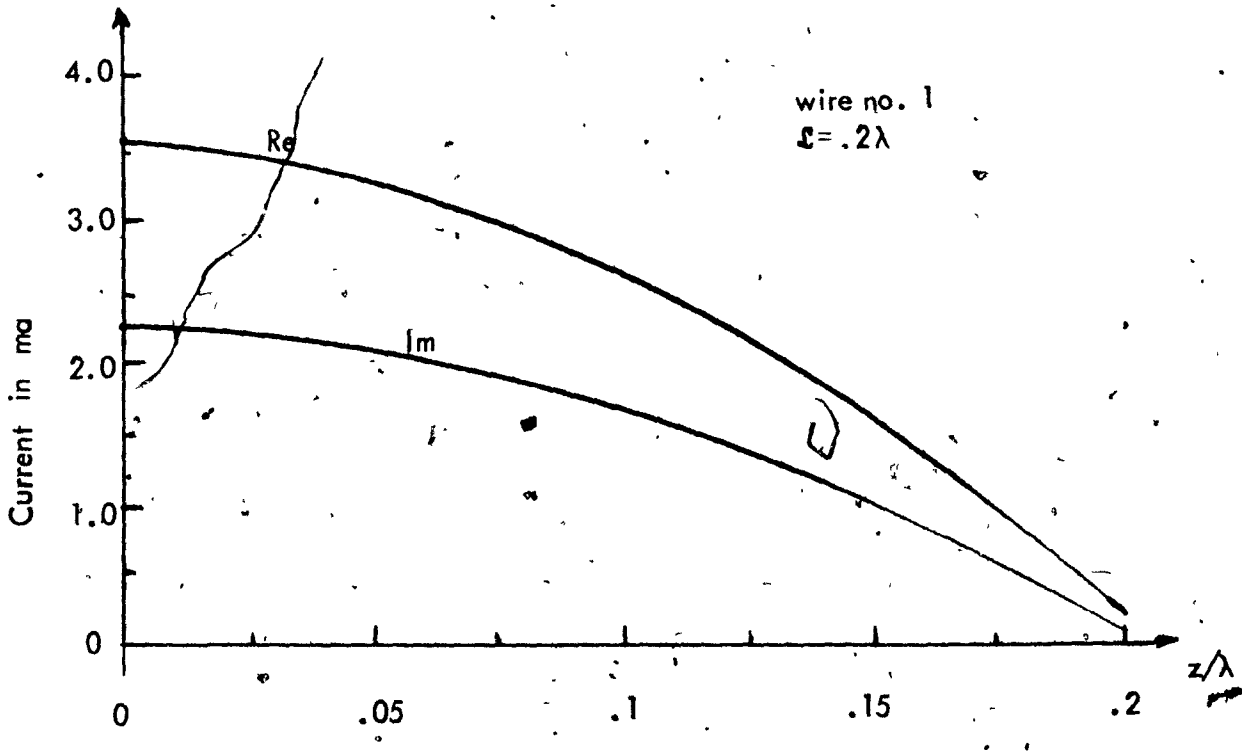
wire no. 1
ℓ = .2λ
Re
Im
Current in ma
4.0
3.0
2.0
1.0
0
0
.05
.1
.15
.2
z/λ

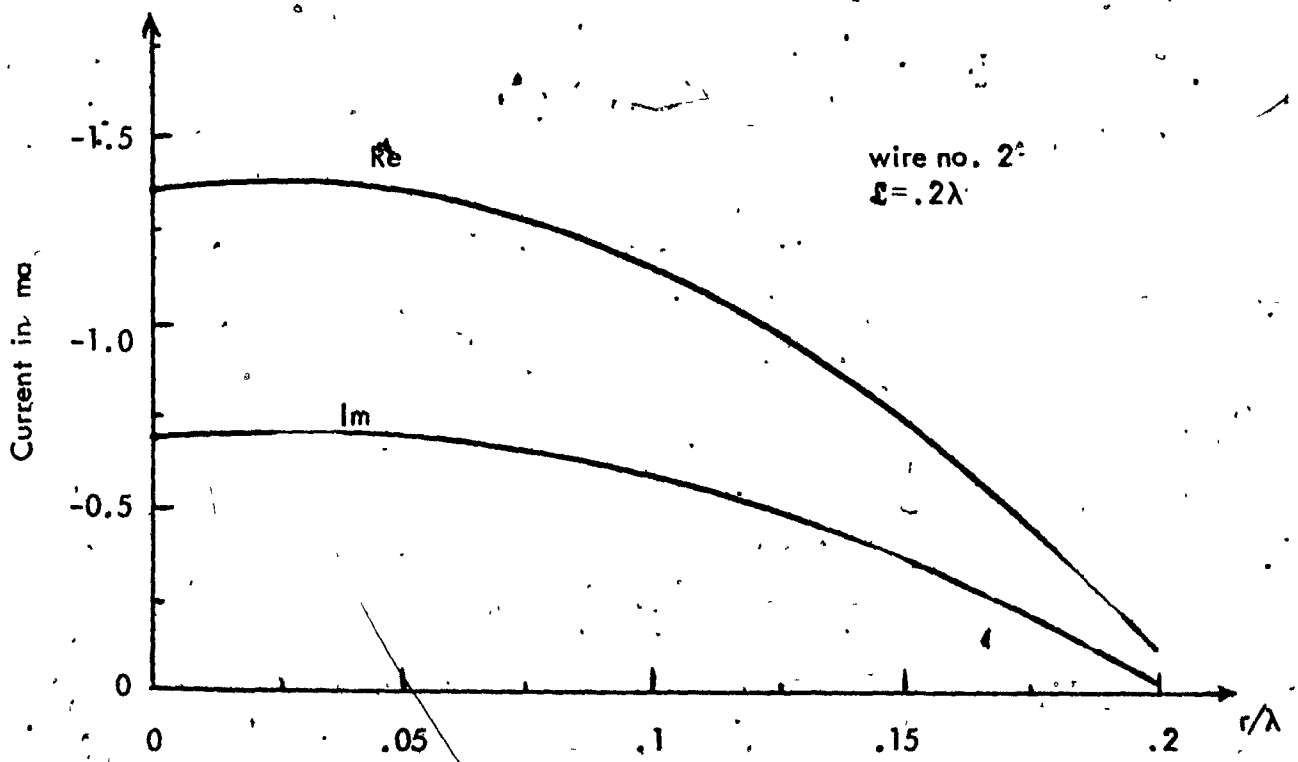
wire no. 2
ℓ = .2λ
Re
Im
Current in ma
-1.5
-1.0
-0.5
0
0
.05
.1
.15
.2
r/λ

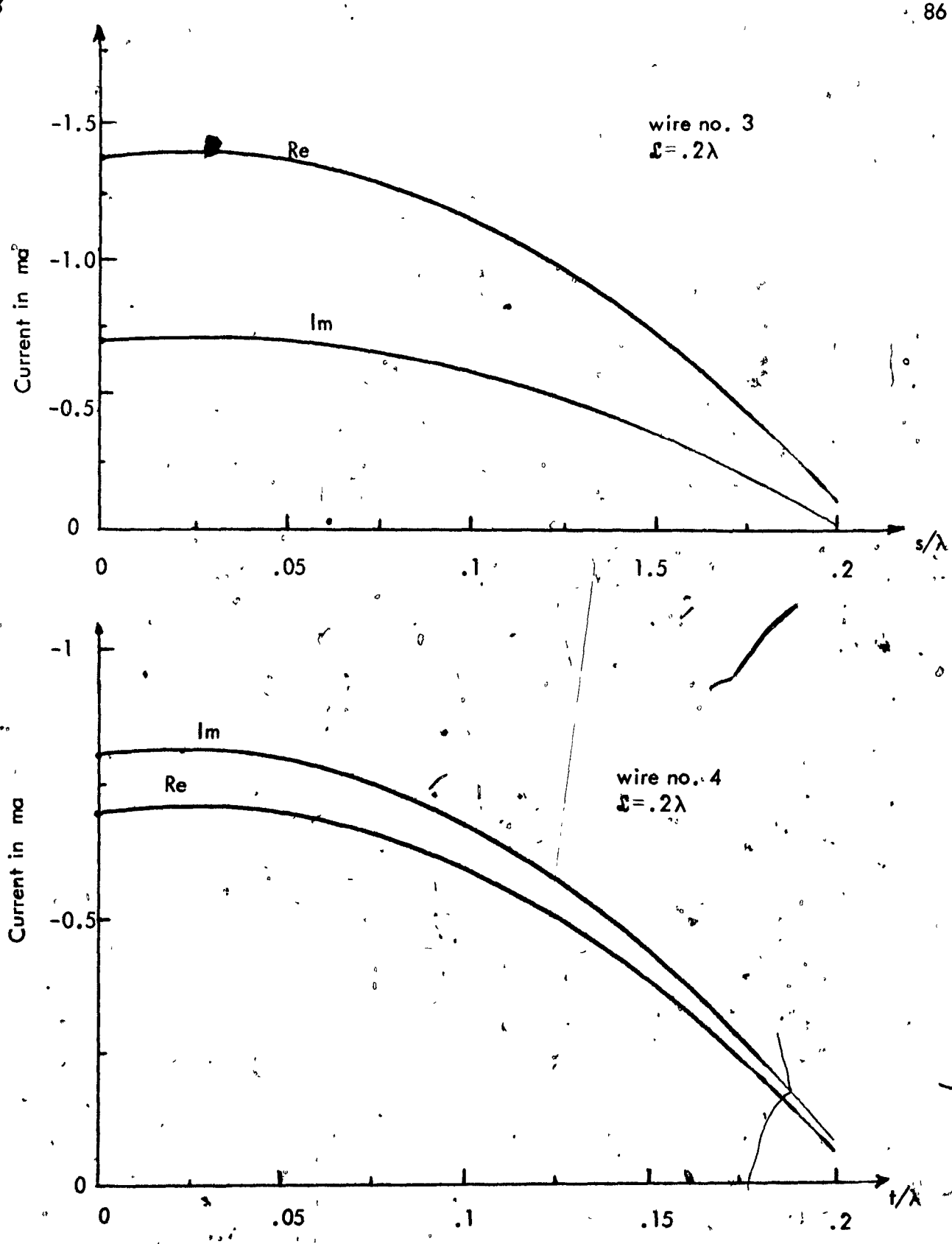

FIGURE 5.18 Current Distribution on a Three Dimensional Brown Wire Scatterer ($a = \lambda/200$).

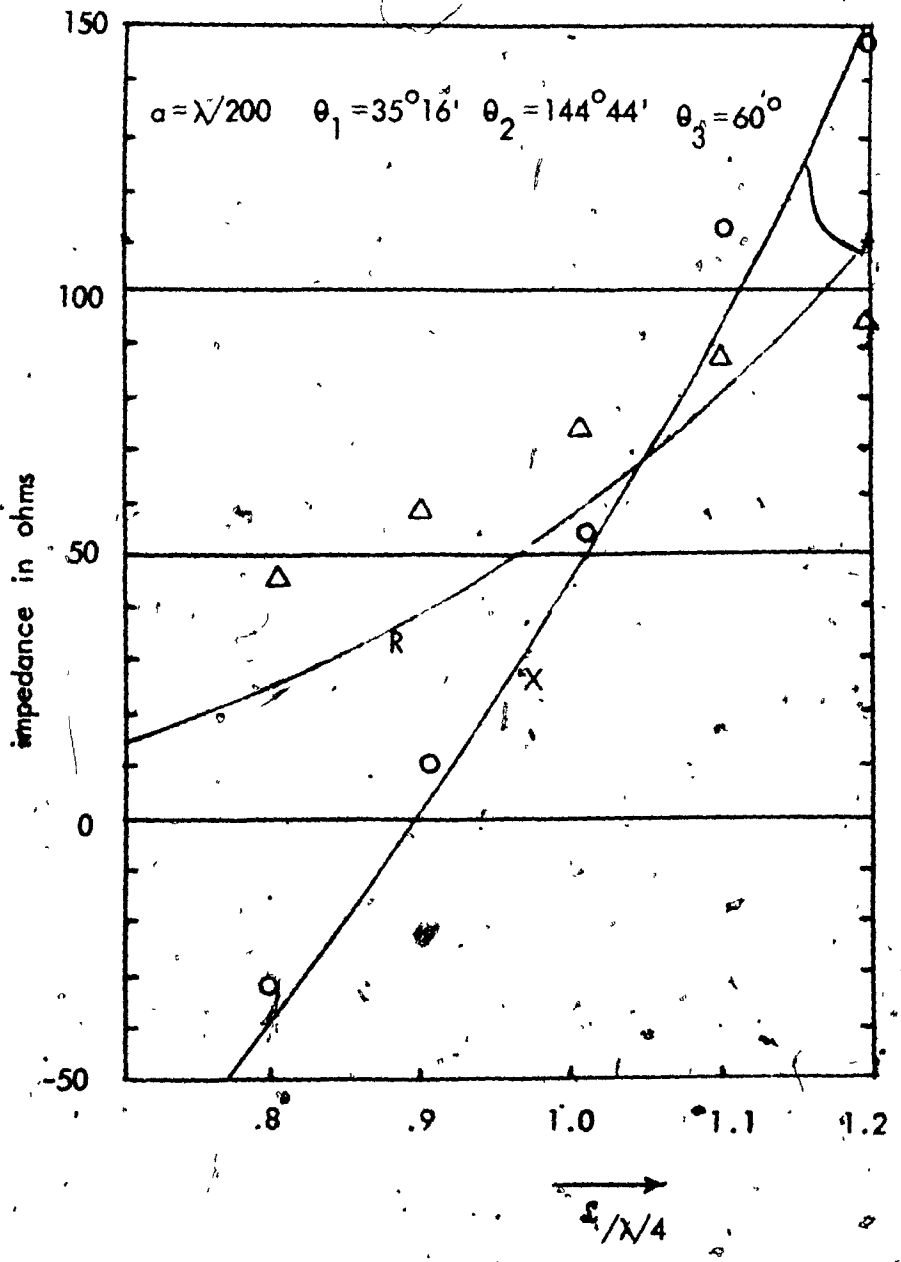

FIGURE 5.19 Theoretical and Numerical Values of Input Resistance R and Input Reactance X of Brow Wire Configuration.

—— Theoretical Method

OOO
ΔΔΔ This Method

CHAPTER VI

CONCLUSIONS

In this thesis, an arbitrary interconnected straight wire structure, illuminated by a uniform plane wave linearly polarized, was analysed. Problems in which the angle between the wires is as small as 2° and as large as 178°, have been successfully solved for the current distribution on the wires. These problems have never been solved before. The collinear wire problem was also discussed.

The far scattered field, the bistatic radar cross-section and the mutual impedance have been computed for some configurations of engineering interest. Excellent agreement with other methods was obtained.

REFERENCES

[1] Butler, C.M., "Currents Induced on a Pair of Skew Crossed Wires", IEEE Trans. on A. and P., AP-20, no. 6, pp. 731-736, Nov. 1972.

[2] Chao, H.H., Strait, B.J., "Computer Programs for Radiation and Scattering by Arbitrary Configurations of Bent Wires", Scientific Report no. 7 on contract F19628-68-C-0180, AFCRL-70-0374, Sept. 1970.

[3] Chao, H.H., Strait, B.J. Taylor, C.D., "Radiation and Scattering by Configurations of Bent Wires with Junctions", IEEE Trans. on A. and P., AP-19, no. 5, pp. 701-702, Sept. 1971.

[4] Chan, K.K., "Galerkin's Method for Wire Antennas", M.Eng. thesis, McGill University, 1971.

[5] Chan, K.K., "Projective Solution of Antenna Structures Assembled from Arbitrarily Located Straight Wires", Ph.D. dissertation, McGill University, 1973.

[6] Harrington, R.F., "Matrix Methods for Field Problems", Proc. IEEE, vol. 55, no. 2, pp. 136-149, Feb. 1967.

[7] Harrington, R.F., "Field Computation by Moment Methods", The Macmillan Company, N.Y., 1968.

[8] Harrington, R.F., and Mantz, J.R., "Strait Wires with Arbitrary Excitation and Loading", IEEE Trans. on A. and P., AP-15, no. 4, pp. 502-512, July 1967.

[9] Hildebrand, F.B., "Introduction to Numerical Analysis, McGraw Hill, N.Y., pp. 319-325, 1956.

[10] Kuo, D.C., Strait, B. J., "Improved Programs for Analysis of Radiation and Scattering by Configurations of Arbitrarily Bent Thin Wires", Scientific Report no. 15, on contract F19628-68-C-0180, AFCRL-72-0051, Jan. 1972.

[11] Krasnosel'skii, M.A., et al, "Approximate solution of Operator Equations", Wolters-Noordhoff publishing, Groningen, 1972.

[12] Mei, K.K., "On the integral equations of thin wire antennas", IEEE Trans., 1965, AP-13, pp. 374-78.

[13] Popovic, B.D., "Polynomial Approximation of Current Along Thin Symmetrical Cylindrical Dipoles", Proc. IEE, vol. 117, no. 5, pp. 873-878, May 1970.

[14] Popovic, B.D., "Analysis of Two Identical Parallel Arbitrarily Located Thin Assymmetrical Antennas", Proc. IEE, vol. 117, no. 9, pp. 1735-1740, Sept. 1970.

[15] Prasad, S., and King, R.W.P., "Experimental Study of Inverted L, T and Related Transmission Line Antennas", J. of Res. of the N.B. of Standards, Radio Propagation, vol. 65D, no. 5, Sept.-Oct. 1961.

[16] Richmond, J.H., "Digital Computer Solutions of the Rigorous Equations for Scattering Problems", Proc. IEEE, vol. 53, pp. 796-804, 1965.

[17] Sayre, E.P., "Junction Discontinuities in Wire Antenna and Scattering Problems", IEEE Trans. on A. and P., AP-21, pp. 216-217, 1973.

[18] Silvester, P. and Chan, K.K., "Bubnov-Galerkin Solution to Wire Antenna Problems", Proc. IEE, vol. 119, pp. 1095-1099, 1972.

[19] Silvester, P. and Chan, K.K., "Analysis of Antenna Structures Assembled from Arbitrarily Located Straight Wires", Proc. IEE, vol. 120, pp. 21-26, 1973.

[20] Simpson, T.L., "Top Loaded Antennas, a Theoretical and Experimental Study", Ph.D. dissertation, Harvard, 1969.

[21] Strait, B.J. and Harrington, R.F., "Analytical and Computer Design of Array Antennas. Analysis and Synthesis of Electromagnetic Scattering Systems", Report, AFCRL-TR-73-0080, 1973.

[22] Strait, B.J., Sarkar, T., Kuo, D., "Special Programs for Analysis of Radiation by Wire Antennas", Scientific Report no. 1 on contract F19628-73-C-0047, AFCRL-TR-73-0399, June 1973.

[23] Strait, B.J., Hirasawa, K., "Computer Programs for Radiation, Reception, and Scattering by Loaded Straight Wires", Scientific Report no. 5 on contract, F19628-68-C-0180, AFCRL-70-0108, April 1969.

[24] Stroud, A.H., Secret, D., "Gaussian Quadrature Formulas", Prentice Hall, Inc., Englewood Cliffs, N.J.

[25] Thiele, G.A., "On the Application of the Point Matching Technique to Antenna and Scattering Problems", Ph.D. dissertation, Ohio State University, 1968.

[26] Thiele, G.A., "Computer Techniques for Electromagnetics and Antennas", Part 1, University of Illinois, 1970, (ed.: R. Mittra)

[27] Taylor, C.D., Lin, S.M. and Adam, H.V., "Scattering from Crossed Wires", IEEE Trans. on A. and P., AP-18, no. 1, pp. 133-136, Jan. 1970.

[28] Turpin, R.H., "A basis Transformation Technique with Application to Scattering by Wires", IEEE Trans. on A. and P., AP-20, pp. 80-82, 1972.

[29] Warren, D.E., Baldwin, T.E., Adams, A.T., "Near Electric and Magnetic Fields of Wire Antennas", IEEE Trans. on A. and P., AP-22, no. 2, March 1974.

[30] Nasu, N., "The Input Impedance of the Conical Antenna with V-Elements", unpublished manuscript.